Logged In

~~SECRET~~ SPECIAL HANDLING

AC-04306
VOLUME I
31 March 1965
Copy No. 3

NRO APPROVED FOR RELEASE
DECLASSIFIED BY: C/IART
DECLASSIFIED ON: 9 JULY 2012

Quill

RADAR

PROGRAM [redacted]

VEHICLE 2355 SYSTEM REPORT (U)

VOLUME I – SUMMARY

Quill

BYE 36454/65
~~SH [illegible]~~
SAFSS
Volume I
P-12498
cy 3

~~SECRET~~ SPECIAL HANDLING

LOCKHEED MISSILES & SPACE COMPANY

AC-04306
Volume I
31 March 1965

NRO APPROVED FOR RELEASE
DECLASSIFIED BY: C/IART
DECLASSIFIED ON: 9 JULY 2012

Copy No. 7
______ Sheets

BYE-36454/65 3UOL1L

PROGRAM [redacted]
VEHICLE 2355 SYSTEM REPORT (U)
Volume I - Summary

Contract [redacted]
Supplemental Agreement Number 13

Prepared:

[redacted]

[redacted]
Chief Operations
Program [redacted]

Approved:

[redacted]

[redacted]
Manager
Program [redacted]

Approved:

David D. Bradburn

David D. Bradburn
Lt. Colonel, USAF
SAFSP

BYE 36454/65

FOREWORD

This report covers the span of time from the inception of the first satellite borne radar system through the final evaluation of the on orbit performance of the first flight. An objective review is attempted, of the complete scope of activities associated with bringing a new system into being and of the system performance during an essentially nominal and troublefree mission.

From this review, it is hoped that the systems management and program control parameters which were found to be effective may be properly recognized and thereby enhance the organization and conduct of similar future activities.

The system definition and resulting configuration is reviewed in retrospect, together with the problems associated with this Program development and testing.

The engineering management concept and the test philosophy which were applied are outlined and restated, with the objectives of first recording these, and then attempting to objectively analyze them for areas susceptible to improvement. The Air Force - LMSC - Associate Contractor team is defined, as it existed during the development, testing and operation of Vehicle 2355.

The system performance from launch through recovery and thence to battery depletion is evaluated from the primary aspect of payload operation.

System performance is compared against predictions, and the performance accomplishments and achievements are enumerated.

The report is therefore, in addition to a flight report, a total summary of the composite effort associated with the preparation and operation of this system. From the system evaluation certain conclusions and recommendations are formulated which are intended to be useful for later work on similar systems.

Through the medium of the detailed information contained in this report, it is intended to properly acknowledge the efforts of all those who were instrumental in managing and conducting a program which produced a completely successful mission with the first flight of a new payload vehicle system.

PART I

Table of Contents

Report Numbering and Organization

The complete 2355 System Report is contained in three volumes.

Volume I - (PART I) - Summary
Volume II - (PART II) - Engineering
Volume III - (PART III) - Flight Performance

The report paragraph numbering is in accordance with the following convention:

First number indicates volume number
Second number indicates main paragraph number
Third number indicates a subparagraph
Fourth number indicates a further subdivision of a subparagraph

Figures are numbered consecutively within main paragraphs.

Reports By Participating Contractors

The complete system description and performance evaluation is contained in reports issued by the three contractors. These are listed here for reference by the reader:

Lockheed Missiles and Space Company:

Title: 2355 System Report, dated 31 March 1965.

Volume I - Summary
Volume II - Engineering
Volume III - Flight Performance

Goodyear Aerospace Corporation:

Title: Program Report, KP-II Orbital Doppler Radar, Thor/Agena Satellite Program, dated 1 March 1965.

[redacted]

Title: [redacted]

PART I

Report Abstract

1.1 INTRODUCTION

This report is divided in three parts. Part I is an abstract containing those system parameters and performance factors of principal interest to a reader whose time may not permit a thorough review of the entire report. The System Description and System Performance are treated in much greater detail in Part II and Part III respectively; however, Program Management-Background, Program Objectives, Mission Description and Conclusions and Recommendations are contained entirely in Part I. The high interest content of the radar imagery dictated placing extensive examples in Part I. The fine resolution radar imagery, the imagery of engineering interest and the summary of data and performance pertaining to each item were provided for the System Report by the [redacted] Grateful acknowledgment is made for this contribution.

Part II is devoted to the technical aspect of the program development and discusses primarily those items which were peculiar to the satellite application of the radar payload. An adequate knowledge of the basic Agena vehicle and subsystems is assumed. In the course of solving the several developmental problems which were encountered - mounting of heavy and dense components, high voltage power supplies, fine attitude control, use of a wide band video data link, a new radar antenna design and the associated flight sciences work - studies and research of a significant magnitude were conducted. It has been an objective in the preparation of Part II to allow the engineering personnel who were involved in these development problems to record the effort and results in a manner which they considered most significant and valuable, utilizing as guidelines the statements contained in the Foreword. Extensive basic data is included in this report, which was deliberately intended to be of a much broader and more thorough scope than a normal flight report. The payload is described in this Lockheed report in more detail than are the other subsystems, by use of excerpts from the Goodyear Aerospace Corporation Program Report. The test sequences and schedules which resulted therefrom are included for record purposes. The Air Force program management was extremely capable and knowledgeable of all details causing program delays. The resulting direction given to the participating contractors permitted the orderly solution of the problems and produced a system capable of predictable operation in orbit.

Part III generally follows the format of Part II in recording orbital performance data by subsystem. The principal section of Part III, Para. 3.4, is utilized as an archive for payload orbital data. The data included in Part III has been as extensive as the economics of time and effort would permit.

1.2 Program Organization

1.2.1 Program Management - Background

Based on an earlier proposal to the Air Force, Lockheed Missiles and Space Company was awarded a contract in November 1962, to place in orbit a coherent, side-looking radar system. The contract specified that Lockheed (System Associate Contractor) would provide overall systems engineering and technical direction of the program, as well as the Agena and its various subsystems (power, command and control, telemetry, etc.). [redacted] (Eastern Associate Contractor) was made responsible for designing the experiment, designing and constructing the optical correlator for processing the raw radar data, and evaluating the data obtained from the experiment. Goodyear Aerospace Corporation (Associate Contractor) was assigned the task of providing the payload hardware as well as participating in the experiment design, test and operation. The contract specified that two vehicles should be launched (2355 and 2356). The payload for 2357 was to be prepared. The payloads of each of the vehicles were to be essentially identical; the first vehicle originally was scheduled to be launched in April 1964. Figure 1.2.1.1 depicts the program management structure.

1.2.2 Contractor Responsibilities

1.2.2.1 Lockheed - System Associate Contractor - was assigned the responsibility of providing System Engineering and Technical Direction to the P-40 Program, subject to the overall management of the Secretary of the Air Force, Special Projects (SAFSP).

In addition to system management the Program Office was responsible for

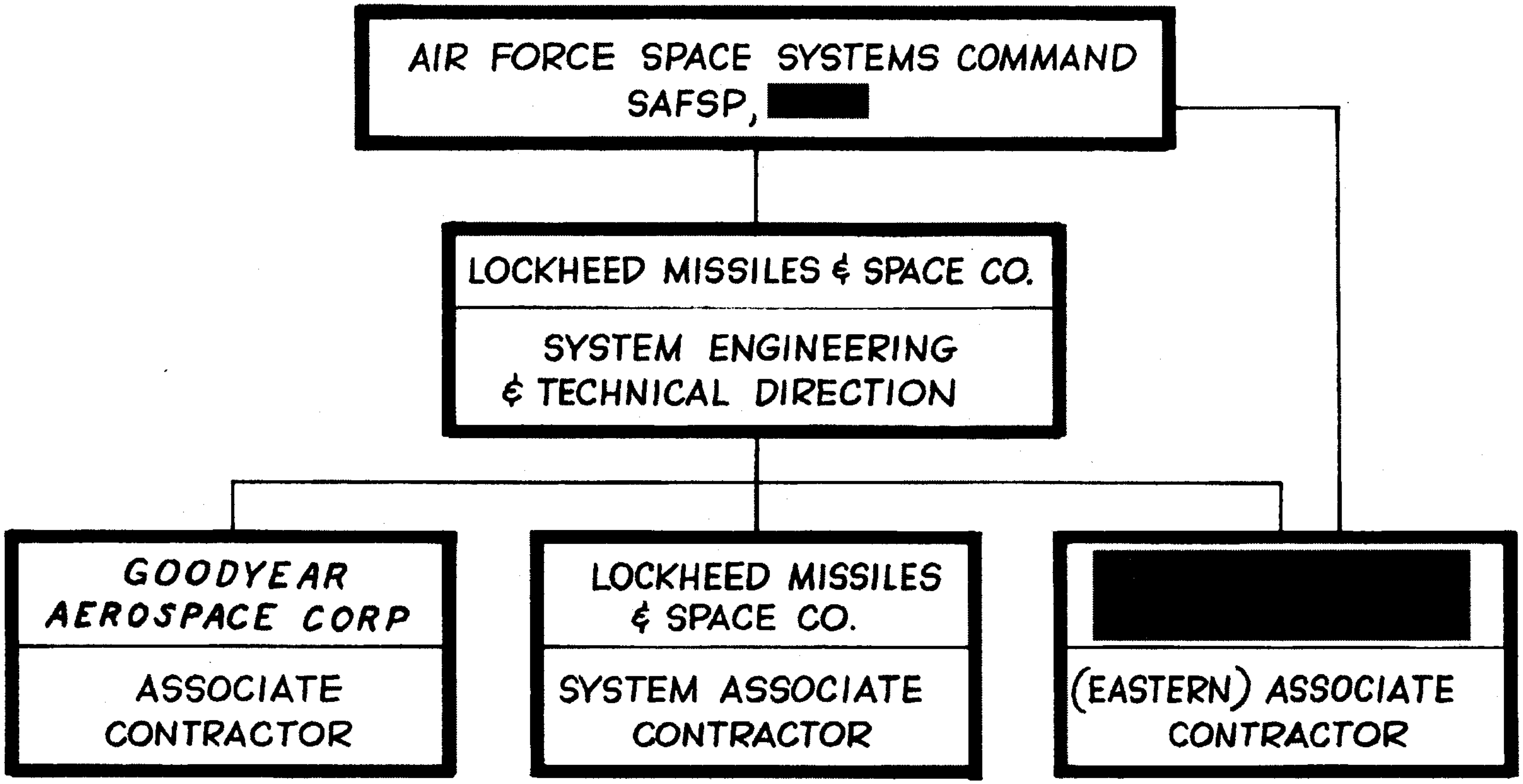

Figure 1.2.1.1 Program Management

coordinating all activities of the three Associate Contractors to insure a technically compatible program to meet planned objectives.

Responsibilities assumed by Lockheed to integrate all activities as necessary to achieve all flight objectives included, but were not limited to, the following:

- o Perform technical direction and engineering management within the parameters as established by SAFSP.
- o Determine system requirements and establish system performance through a coordinated study and analysis endeavor.
- o Recommend to SAFSP, the required research, development and experimentation to achieve program objectives.
- o Prepare the requirements for, and evaluate the Design Control Specifications, Acceptance Test Specifications, Engineering Analysis Reports, Test Procedures, and Specifications, by coordinating total effort with the Associate Contractors.
- o Analyze and make recommendations to the Air Force, as required, on System, Subsystem and Component development and test programs.
- o Establish a Systems Engineering and Technical Direction (SETD) capability to conduct continuous evaluation of equipment performance to determine the degree of compliance with all system functional and operational requirements.
- o Hold SETD meetings with Associate Contractors to coordinate latest changes necessary to meet program objectives, by performing technical evaluations of requests from the Associate Contractors for

design or performance waivers on components, subsystems, end item equipment, and ground support equipment, making recommendations to SAFSP regarding approval of changes.

- o Review, analyze and make recommendations to achieve interchangeability and compatibility of associated subsystem and equipment designs formulated by Associate Contractor.
- o Review the reliability programs established by the Associates to assure consistency, quality and adequacy of effort.
- o Assist Program management in determinimg Program milestones, design parameters, procurement techniques and releases.
- o Integrate AGE, GHE, Spares and all necessary flight support equipment to provide flight test vehicle and flight vehicle readiness.
- o Perform the necessary techniques for integration of GAC Radar equipment with LMSC payload antenna.
- o Perform qualification tests on payload system consisting of radar subsystem, space structure subsystem and recovery subsystem.
- o Provide the necessary assistance in pre-flight planning and programming, in-flight support analyses, post-flight T/M analyses and preparation of preliminary and final ephemeris.
- o Prepare and release a final System Report.

1.2.2.2 Goodyear Aerospace Corporation was assigned responsibilities as an Associate Contractor to fulfill the following requirements to meet the P-40 Program objectives:

- o Perform the necessary functions to accomplish the design, development, procurement, manufacture, and development testing of the radar subsystem, not including the antenna, takeup reel, data link, interconnecting cabling, or the waveguide.

- o Design, develop and provide the necessary ground support equipment to meet the Program objectives, including all payload test equipment for payload units and system test sets for the payload as a subsystem.
- o Participate in the radar subsystem acceptance at LMSC facility.
- o Perform the retrofits, modifications and maintenance of the radar subsystem.
- o Recommend readiness and provide certification of the radar subsystem prior to systems test and launch.
- o Furnish wooden mock-ups for LMSC integrated mockup.
- o Perform the development and acceptance testing of the radar subsystem.
- o Assist in the qualification testing of the payload system in regard to the radar subsystem at Lockheed. Perform the necessary payload qualification at Goodyear.
- o Recommend and provide the necessary spares for the radar subsystem to give adequate backup to the Program.
- o Determine the need for, and provide the necessary tools, jigs, and similar items needed to install, check and adjust all components, subassembly, and assembly of the radar subsystem during the subsystem assembly and checkout.
- o Provide film recorders for tracking station data link recording.

- Assign field personnel to LMSC to assist in performing the necessary modifications and tests to assure technical integrity and technical capability of the radar subassembly and payload vehicle.

1.2.2.3 [redacted]

[redacted] was assigned responsibilities as an Associate Contractor to perform the following tasks:

- Provide technical advice and assistance to Lockheed Missiles and Space Company and Goodyear Aerospace Corp., in the areas of payload design and establishment of system requirements for flight operation.
- Design and build an advanced optical correlator for processing the payload data.
- Process (correlate) the payload data from the recovery capsule and the wideband data link.
- Perform payload data analysis and evaluation, including system performance evaluations against predictions.
- Issue a comprehensive report covering all work performed.

1.2.3 Security

The Program requirements for security were established by SAFSP [redacted] and are graphically portrayed in Fig. 1.2.3.1, Security Concept, on the next page.

NRO APPROVED FOR RELEASE
DECLASSIFIED BY: C/IART
DECLASSIFIED ON: 9 JULY 2012

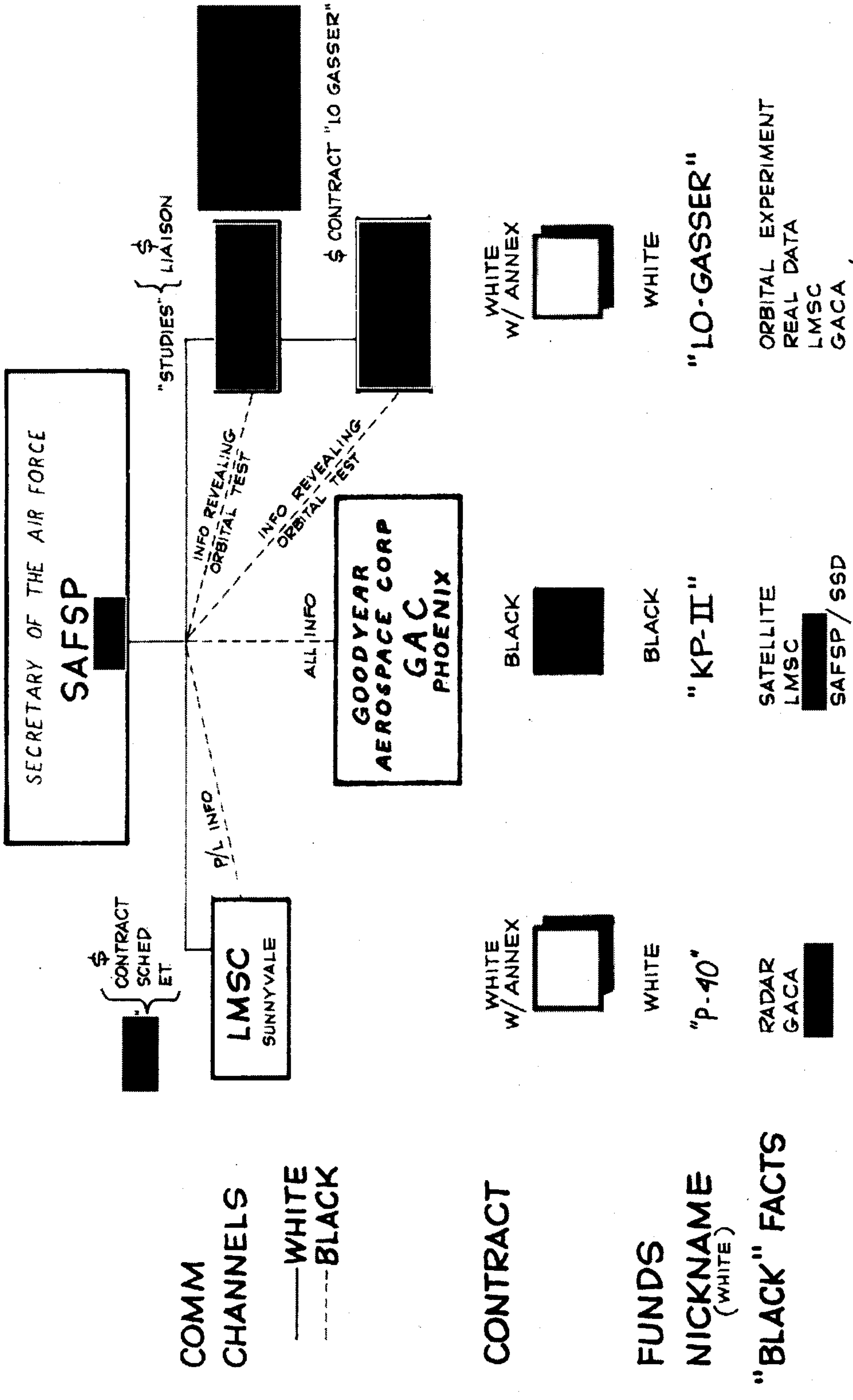

Figure 1.2.3.1 Security Concept

1.3 Program Objectives

Primary Mission Objective The primary objective of the orbital flight was to demonstrate that a fine-resolution radar strip map of a portion of the earth's surface can be generated through use of a satellite-borne synthetic-aperture radar system. For the purpose of this demonstration a resolution goal of 50 feet in azimuth and in slant range was established.

Secondary Mission Objectives A number of secondary objectives of scientific and/or engineering significance were also established. Among these are the following:

- Quantitatively evaluate the performance of the radar system, with emphasis on azimuth-dimension behavior:
- Determine the performance limits imposed by:
  - Payload design parameters
  - Payload in-flight performance
  - Vehicle attitude behavior
  - Atmospheric conditions
  - WBDL design and performance
- Determine the reasons for any observed anomalous performance of the system:
- Collect data on target-field reflectivity.
- Develop engineering data useful for aerospace radar system designs.
- Demonstrate the capability of the ground recording equipment to record useful data received via the WBDL.

Primary Vehicle Objectives The launch phase primary vehicle test objective was to inject the Agena (SS-01A) into a near circular orbit so that the satellite altitude would be 130 ± 13 nautical miles when passing between 30°N and 70°N geodetic latitudes with an orbit plane inclination of 70 ± 0.25 degrees.

The orbit phase primary vehicle test objectives were:

- To maintain, during the minimum orbit life of 65 orbits, a stabilized horizontal attitude with the following tolerances (-Z axis up and -X axis forward):
  - Deadband 0.15 ± 0.07 degrees, all axes
  - Bias uncertainty ± 0.4 degrees, all axes
  - Maximum pitch rate 0.002 degrees/second
  - Maximum roll rate 0.005 degrees/second
  - Maximum yaw rate 0.003 degrees/second
- To yaw the vehicle to a bias angle of 2.44 ± 0.3 degrees to the left and to the right in response to commands.
- To provide electrical power to sustain payload and vehicle life for a minimum of 65 orbits.
- To command and control vehicle and payload operation.
- To obtain data required for the generation and verification of commands to control vehicle and payload operation.

The recovery phase primary vehicle test objectives were:

- To orient the SS-01A to a proper nose down attitude, separate the recovery capsule at the proper time and provide retro-thrust to the capsule so that its re-entry trajectory falls within a predetermined recovery area.

- To recover the recovery capsule with its payload by air or surface units deployed for that purpose.

1.4 Mission Description

The mission of Vehicle 2355 was to place in orbit a coherent X-Band, side-looking radar system payload in order to obtain a high resolution terrain map. The payload was to be operated in realtime under command of the Vandenberg and New Hampshire Satellite Tracking Stations. Operation of the payload was to be limited to the Continental United States. The SS-01A vehicle was to be injected into a near circular orbit so that the altitude over the areas to be recorded would be approximately 130 nautical miles. Precise attitude stabilization of the vehicle would then orient the radar antenna so that the main lobe of the radar beam would be at a fixed depression or look angle of 55° from the horizontal, thereby illuminating a swath approximately 10 nautical miles wide at a distance of 93 nautical miles to the left of the satellite ground track.

The data obtained from the payload was in the form of target echoes which were synchronously demodulated to preserve both phase and amplitude of the signals. These signals, which constitute the raw radar map Data or doppler history of the illuminated terrain, were recorded photographically on film in a recoverable capsule aboard the satellite. Simultaneously, these signals were transmitted over the Wide Band Data Link to the tracking stations where they were again recorded photographically on film by ground based recorders and also electronically on wide band magnetic tape recorders. The film recorded in the satellite was to be recovered in the Pacific Ocean area by means of air catch of a recovery capsule. Figure 1.4 portrays the payload operating swaths and the tracking stations zero and five degrees elevation circles of coverage.

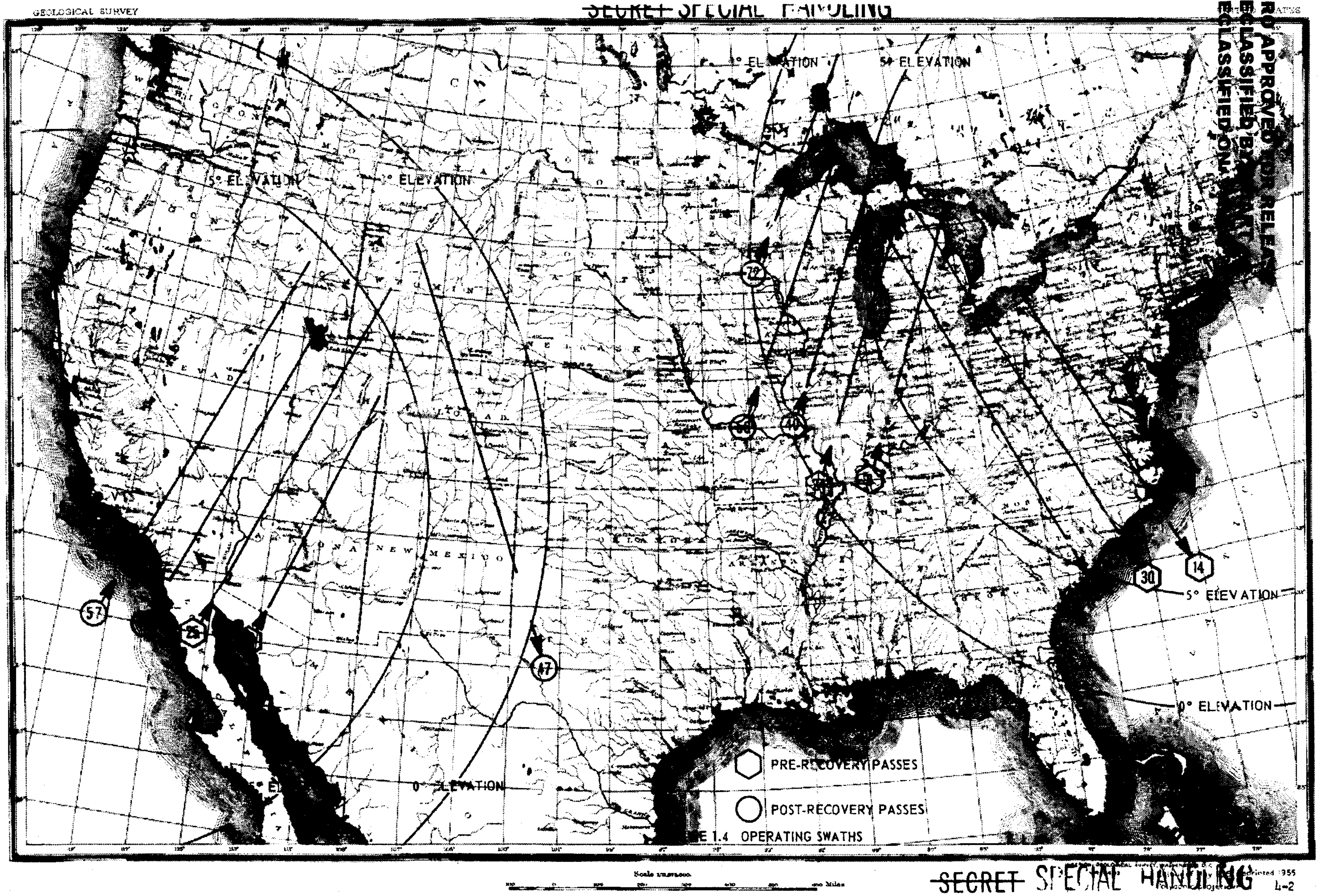

E 1.4 OPERATING SWATHS

1.5 System Description

The satellite vehicle utilized for this mission consisted of the following subsystems:

Subsystem A (SS/A) - Structural
Subsystem B (SS/B) - Propulsion
Subsystem C (SS/C) - Electrical
Subsystem D (SS/D) - Guidance and Attitude Control
Subsystem C & C - Command and Control
Payload Subsystem
Recovery Subsystem

The above subsystems are described in some detail in Part II, Para. 2.1, Satellite System Engineering; Para. 2.2, Radar Payload; and Para. 2.3, Test, for the Recovery Subsystem. Since the Recovery Subsystem was GFE, the effort was limited to test on that subsystem, and the configuration description is confined to the information considered necessary for understanding of system operation.

The satellite structure forward of the standard Agena vehicle interface housed and supported the guidance system components, the radar payload and associated power equipment and the recovery capsule.

The radar payload was developed for satellite application by Goodyear Aerospace Corporation from the AN/UPQ-102 side looking doppler radar utilized in the RF-4C aircraft. The radar components include: (1) a Transmitter-Modulator, which is basically a high power R.F. pulse amplifier; (2) an RF-IF unit, which generates a low power RF pulse for the transmitter and receives and compresses the reflected radar pulse; (3) a Reference Computer which generates timing and control signals, RF pulses for transmission, synchronously demodulates the received intermediate frequency to provide video data and performs electronic beam steering to a zero doppler position; (4) a Power Control Unit, which controls and switches power and generates regulated voltages necessary for the radar; and (5) a Recorder which records the received video from the Reference Computer on film by exposure from the face of a cathode ray tube. The film, containing the doppler history of each target, is returned by the recovery capsule. Simultaneously the video data from the Reference Computer is transmitted by means of an R.F. data link to the tracking stations, and recorded in a similar film recorder.

The high power output pulse of the radar was transmitted through a flat, phased array, antenna mounted on the side of the satellite with the beam oriented perpendicular to the vehicle longitudinal axis and at a 55 degree depression angle below horizontal. The beam width was .346 degrees in the azimuth direction and 2.9 degrees in the vertical direction at the half power points. The satellite was rotated 180 degrees after injection into orbit (positioned for recovery pitch down) and was stabilized in a horizontal plane. During the payload operating passes the horizon sensors were disconnected and the satellite was precisely stabilized under fine attitude control by the inertial reference package gyros. The system was supplied electrical power by three silver-zinc batteries, the output of which was converted and regulated as required. The electrical capacity of the batteries limited the duration of the mission. The vehicle was commanded through an S-Band beacon and returned data through two VHF telemetry links and the wide band UHF data link.

After separation of the recovery capsule the vehicle was re-stabilized in the horizontal plane and the payload was operated through the data link until power depletion on orbits 72 - 73. The orbit decayed and the vehicle re-entered on orbit 333 at 1027Z, 11 January 1965.

1.6 System Performance - The system performance was faultless throughout the orbital mission, until battery depletion on Orbit 72 - with the exception of minor unexplained voltage disturbances on Orbits 8 and 9. This section presents the significant payload operating information, radar imagery samples and discussions of the payload performance, preceded by a brief summary of system parameters and performance.

Launch

Date: 21 December 1964 Time: 1908:56Z
Location: Launch Complex 75-1-1, Vandenberg AFB
Vehicle: LV-2A #425 SS-01A #2355

Orbit	Predicted	Actual
Period (MIN)	89.44	89.66
Perigee (N.M.)	130	135.82
Apogee (N.M.)	154	157
Inclination (deg.)	70.0	70.11
Eccentricity	.003	.0036
Active Orbits	65	73
Recovery	65	33
Payload Operations	13	14

Area recorded as fine resolution radar imagery:
approximately 70,000 square miles (nautical).

1.6.1 Evaluation of Radar Imagery

General Comments - An extensive amount of recorded video data was generated by the flight of vehicle 2355; this data has been processed to generate fine-resolution radar imagery. Examples of this imagery have been selected for the purpose of illustrating the radar-appearance of various cultural targets and non-cultural terrain areas which fall within the imaged swaths, as well as to illustrate system phenomena of engineering interest. A detailed evaluation of the results of the radar experiment which culminated in the 2355 flight is being prepared under separate cover by The [redacted] the results presented in this volume are of a preliminary nature and therefore somewhat incomplete. In examining the incorporated imagery, the reader must keep in mind the fact that the photographic prints in this report do not permit the full azimuth resolution and dynamic range capabilities of the system to be preserved; these are considerably better preserved in the high-quality photographic transparencies which have been generated during the program, and are at their very best at the output of the optical data processor prior to photographic recording. The processor output may be viewed by the user of the radar imagery, without recording, in situations where the full resolution and dynamic range must be preserved.

The first eleven examples of radar imagery, Figures 1.6.1 through 1.6.11, have been selected to show a reasonably wide variety of cultural and terrain features. Their image quality is typical of the entire mission; these samples have been selected because their content is representative of areas of potential military interest. These first eleven images were all generated from the physically-recovered video data. Corresponding U. S. Geological Survey maps are presented with the radar imagery in instances where this is useful.

Figure 1.6.12 is generated from video data transmitted via the WBDL coincident in time with the generation of the data film used to generate Figure 1.6.11; this comparison permits the effects of the data link on image quality to be observed. Figure 1.6.13 was generated from the same video data which had been stored, upon reception via the WBDL, using the AMIE tape recorder, and then played back onto the same ground-based photographic recorder used in the generation of the Figure 1.6.12 data. The comparison of Figure 1.6.12 and 1.6.13 permits an evaluation of the effects of the AMIE to be made.

Figures 1.6.14 through 1.6.20 illustrates effects which are primarily of engineering interest in providing data for the efficient design of future systems. One of these also shows the effects of severe weather on the radar performance.

A brief discussion of the effects of certain system behavior on image quality is necessary, prior to presentation of the image samples.

Payload Behavior - The radar payload itself performed within nominal specification limits during the generation of the imagery presented in this section. The payload variables which were the key factors in determining image quality were:

- Time coincidence of the CRT sweep with the returns from the most strongly illuminated portion of the terrain; that is, from the terrain lying between the upper and lower 3 db directions of the illuminating beam. Adjustment of the prf is used to effect this coincidence;
- Behavior of the clutterlock oscillator in response to initial attitude of the vehicle at turn-on, and to subsequent angular rotations and accelerations of the vehicle; and
- Behavior of the AGC circuit in response to various target distributions.

Image quality is of course also dependent upon local terrain reflectivity and atmospheric conditions, but these are not controlled payload variables.

Vehicle Attitude Behavior - The attitude orientation of the vehicle at the time of payload turn-on and its subsequent behavior during the payload operating time affect image quality, part of the effect being somewhat indirect. Roll behavior manifests itself in a different manner than do pitch and yaw behavior.

Since the radar is sidelooking, to within a few degrees of normal to the local inertial velocity vector, the roll attitude determines the ground swath which is illuminated. In the payload subsystem as implemented, one is then faced with the problem of selecting a prf appropriate to the resulting slant range from vehicle to swath center, in order to have return video coincidence with the range gate of the receiver and recorder. Roll excursions which are small compared with the elevation beamwidth are of little consequence once the correct prf is established, and larger roll excursions can be tolerated if one is willing to make a prf-adjustment. The prf-setting problem will be covered in further detail in a later paragraph.

The pitch and yaw attitudes of the vehicle at payload turn-on determine the position of the doppler spectrum of the video return. It is necessary to control the position of the spectrum center in order to guarantee proper sampling of the doppler-shifted video while minimizing the generation of ambiguous target responses; this is effected through use of a voltage-controlled oscillator driven by the output of the clutterlock integrator. At turn-on, the random yaw and pitch biases in general cause the doppler spectrum to be misaligned with respect to its proper location, and the voltage-controlled oscillator responds to correct the error. Similarly, this oscillator also responds to pitch and yaw velocities and accelerations subsequent to turn-on. Because the electrical phase center of the antenna is close to the vehicle's mass center, the angular motions of the vehicle do not directly inject phase errors into the video return; therefore no direct degradation of resolution or image signal-to-noise ratio results from the vehicle rotations. The degradations appear as a consequence of the steering of the voltage-controlled oscillator; this is discussed in the next paragraph. The vehicle attitude control is analyzed in detail in Part II, Par. 3.3.

Clutterlock Behavior - The output of a voltage-controlled oscillator (VCO), whose frequency is determined by the instantaneous output of the clutterlock integrator, is injected into a single sideband (SSB) modulator in the receiver along with the video, the SSB output* then being applied to a synchronous demodulator. The purpose of the clutterlock and VCO is to keep the doppler spectrum of the (corrected) video centered about a predetermined offset frequency. When the instantaneous pitch and yaw orientations of the vehicle are such that the doppler frequency is too large, the VCO is commanded to reduce its frequency to compensate the data, and vice versa. In doing so, it injects a phase error into the target returns while correcting the spectrum position. If the VCO output frequency is constant or changing linearly over the pass length, no deleterious effect on resolution is observed. The output of the clutterlock is constrained from varying rapidly, through use of an integrator with a time costant of the order of a few seconds. The time constant of the integrator is determined on the basis of expected vehicle rotation and angular acceleration rates, the widths of the 3-axis limit cycles, and the radar parameters; the two values available in 2355 were 2.5 and 5 seconds, the former being used in the primary

---

*the upper sideband being employed.

operating mode.

At payload turn-on the initial misalignment of the antenna beam with the zero-doppler direction causes the VCO to be driven toward the correct compensating frequency, at a rate determined by the integrator circuitry as well as the magnitude of the initial error. If the rate of change of frequency is approximately linear at this time then the following occurs:

- o The doppler spectrum is gradually translated, at a constant rate, to its proper position, and unambiguous imagery develops; and
- o The VCO injects a quadratic phase error into the target histories; a processor adjusted for optimum processing on the basis of the video data being collected at this time is then improperly adjusted for later times for which the rate has changed, and defocusing occurs unless a subsequent processor adjustment is made.

Once the initial misalignment error is compensated by the oscillator, the VCO behavior will be dominated by the following factors:

- o The vehicle rotates in 3 axes within certain deadbands; the pitch and yaw rotations translate the doppler spectrum, the clutterlock senses the error and the VCO attempts to compensate for it;

- o Unbalanced torques on the vehicle will cause angular accelerations within the deadbands;
- o Gas-pulse firings at the edges of deadbands will introduce impulsive angular accelerations; and
- o A slow VCO frequency shift is required to correct for earth rotation as a function of latitude.

The rotations and accelerations associated with the deadband behavior will cause phase errors which are relatively high-frequency in nature to be injected into the target histories. The first-order effect will be image defocusing in the azimuth dimension, with attendent resolution degradation unless the processor is appropriately readjusted.

The examination of imagery to determine the effects of vehicle motions and clutterlock behavior is still in process; the results will be covered in the forthcoming [redacted] [redacted] report to be published separately.

Comments on Resolution - A key purpose of the 2355 flight was to demonstrate the realization of fine azimuth resolution using an orbital synthetic-aperture radar system; a great deal of attention was therefore devoted to minimizing errors which would unnecessarily degrade azimuth resolution. The radar system had the inherent potential to achieve resolution somewhat finer than 10 feet in azimuth, provided that atmospheric conditions and system malfunctions did not inject excessive degradations. Range resolution, on the other hand, was limited by the bandwidth of the electronics, which had been patterned after the AN/UPQ-102 radar system for reasons dictated by expediency; the most optimistic estimate of achievable slant-range resolution was of the order of 36 feet, which in turn implied a ground-range resolution of 60 feet at the design depression angle. Improvement of the range resolution to make it comparable with the expected azimuth resolution was not warranted, since it would not have affected the demonstration of the synthetic-aperture feasibility, and would have entailed considerable expense and delay.

The radar imagery generated from video data collected during the 2355 flight has a ground-range resolution of approximately 75 feet, and an azimuth resolution of the order of 10 feet when the processor is optimally adjusted for the particular target area being viewed. As explained above, the behavior of the clutterlock, which in turn responds to vehicle attitude motions and initial conditions, may necessitate repeated readjustments of the processor. In situations where the processor was focused only once near the start of the pass, overall azimuth resolution is typically of the order of 15 to 30 feet. The resolution figures quoted here are applicable to the imagery as recorded, directly at the processor output, on photographic transparency material. The photographic prints shown in this report are limited by the characteristics of the paper to a resolution of the order of 6 lines per mm; at the scales chosen for most of the figures, ground-range resolution is degraded to about 150 feet, and azimuth resolution is degraded to 90 to 100 feet.*

Two independent measures of achieved resolution are available. The first of these is obtained from the imagery of Pass No. 8 itself--a test array of radar corner reflectors at [redacted] fell within the mapped swath. The image of this array showed that azimuth resolution of roughly 10 feet, and ground-range resolution of roughly 75 feet, were

---

*The two figures are different because of the difference in the azimuth and ground-range scale factors in the print.

achieved. The second determination was made via a measurement of the two-dimensional response of the system to a strong isolated target which was imaged near the southern end of Pass 30. The system impulse response determined directly at the output of the optical processor, had a half-power width of 10 feet in azimuth and 72 feet in ground range.

The test-array measurement will be discussed further in Par. 1.6.2 below.

Positioning of the Reflected Energy in the Range Gate - In order to preserve full azimuth resolution and avoid the superposition of undesired azimuth-ambiguous imagery on the desired radar image, it was necessary to employ a radar-repetition rate of the order of 8500 pps, to within a tolerance of perhaps 5 per cent. A pulse was therefore transmitted once every 120 microseconds, to within a few microseconds depending upon the precise value of the prf. At the instant of transmission of any pulse, the previous one had travelled only about 20 nautical miles from the radar en route to the target field, which was typically at a one-way slant range of 170 nautical miles from the vehicle. Under these conditions, about 16 or 17 pulses were making the round-trip between radar and target field at any instant of time; the precise number was dependent upon the precise values of prf and slant range. In a properly designed non-ambiguous system, the return reaching the radar at any instant can only have originated from one particular pulse, not two; this is guaranteed through a proper restriction on the elevation-beamwidth of the radar antenna.
Through a slight adjustment of the inter-pulse period (hence the prf) one may arrange to have the "dead-time" between the arrival of return from two consecutive pulses coincide with the time of transmission of a (later) pulse. In the 2355 system, this was done by choosing one of the 16 available prf

steps, which essentially provided a vernier adjustment on the inter-pulse period. It was furthermore convenient to trigger the CRT sweep in the recorder from the same source which controlled the transmitter timing. The sequence of events was as follows: the radar transmitted a pulse, the receiver and recorder waited 25 microseconds, and the CRT was then swept for 73 microseconds; the system then repeated the cycle after an additional wait of 16 to 24 microseconds (depending on the choice of prf). When the prf was at its optimum value, signal return from the slant range corresponding to the lower half-power point of the elevation beam (the near-edge of the swath) started arriving as the CRT-sweep started, and video from the upper half-power point (the far-edge of the swath) had completed its arrival 73 microseconds later as the sweep was about to be completed.

On certain occasions, the sweep started a few microseconds before the return from the near-range arrived; the imagery corresponding to these occasions lacks contrast and SNR at the near edge, but is better at the far-edge. Conversely, the opposite occured when the sweep was late in starting. On still other occasions, the sweep was begun as the return from the far-edge was arriving, continued while the instantaneous return power level passed through its minimum, and was almost completed by the time return from the near-edge began to arrive; under these conditions, the CRT was inoperative for the major portion of the return, and two strips, inverted with respect to each other, were imaged by the system. Examples of these two classes of situations are shown later. In either event, a slight readjustment of the interpulse time (hence prf) sufficed to re-establish the proper synchronization between the time of arrival of reflected radar energy and the time of initiation of the CRT sweep. The pulse positioning is described pictorially, with additional discussion in Part III, Par. 3.4.4.

AGC Effects - The radar reflectivity of patches of terrain, which vary in character and may or may not include collections of cultural targets, varies over a wide range of values. The spread from the strongest to the weakest reflectivity depends upon the size of the patch one wishes to consider; a typical spread might be of the order of 70 db (i.e., seven orders of magnitude). This 70 db "dynamic range" of the target-field reflectivity distribution exceeds the dynamic range of currently available components in the receiver and recorder chain by some 40 to 50 db. A simple fixed-gain receiver having a necessarily-insufficient dynamic range can be adjusted to operate somewhere between two limiting situations, one in which "strong" targets are handled linearly but "weak" targets and ground-painting are lost, and one in which ground-painting is preserved at the expense of overdriving the circuitry when strong targets are present, this overdriving in turn leading to such undesirable effects as false-target generation and SNR degradation. An AGC provision permits one to adjust gain to match local reflectivity conditions, thereby recapturing some of the advantages of a larger-dynamic range fixed-gain system. The performance of the AGC-equipped radar falls short of that of the latter, however, when very strong and very weak targets are in close azimuth-proximity to each other; the return from the strong targets induces a receiver gain-reduction, and ground-painting and weak targets at nearby azimuth locations are lost. Examples of this effect will be seen later in radar imagery of shorelines. The lack of sufficient dynamic range will also be evident in imagery which contains agricultural areas close to a strong industrial target complex.

Weather - Radar imagery was generated under a wide variety of atmospheric and ground-surface conditions during the 2355 flight. Generally speaking, the northeastern part of the U.S. was experiencing rain, snow, some freezing rain, heavy overcasts and some high clouds during the operation. The ground was wet or snow covered in many areas. Frontal activity was generally weak where present; some imaging through turbulent clouds occurred on Pass 25. In the central Atlantic states the ground was generally drier, although fog and haze were frequently present. Heavy rainfalls were in progress during Pass 16 in Northern California, and had been for several days previously; the ground was flooded in some areas along this pass. In the Southwestern portion of the country, the air was generally clear with the ground in its usual dry state.

As a consequence of this synoptic weather situation, a sampling was obtained of most of the lower-atmosphere phenomena which tend to degrade radar performance. In particular, the presence of widespread light precipitation goes largely undetected in the imagery, and the heavy precipitation along the California coast does not severely obscure underlying structure. The reduction of terrain reflectivity resulting from the wet and snow-covered surfaces was not sufficient to cause obscuration of surface details, although the ground-painting signal-to-noise ratio was undoubtedly reduced as a result of these conditions. One notable omission in the sampling of weather conditions stems from the fact that no strong frontal activity or unstable air masses were present along the flight paths; effects which might be associated with summer storms were therefore not observed.

A more detailed analysis of the weather situation will be presented in the final evaluation report to be released by [redacted]

1.6.1.1 Typical Imagery - The following examples of imagery were generated from physically-recovered video data, and are typical of the recovery results obtained on the first seven operating passes. The processor was optimized for each image to the extent possible. The remarks made earlier with respect to resolution and dynamic range must be repeated here: the paper prints degrade resolution in both dimensions for the scale factors appropriate to this report, and cannot preserve, at any scale factors, the dynamic range available in the optical image at the processor output prior to recording, or in the photographic transparencies generated by this optical image.

The imagery presented in this section is intended for viewing with orientation shown in Figure 1.6.0; it can easily be seen through an examination of Figure 1.6.6 that this orientation preserves a natural appearance of relief in mountainous regions. Increasing system time corresponds to motion from right to left along the image*. The times of various events have been established to within 0.1 second relative to the system time.

---

*The increase of system time from right to left is a necessary consequence of illuminating a swath to the left of the vehicle's ground track, if we also wish to preserve the usual clockwise sequence of the North, East, South and West cardinal directions. A system which looked to the right and preserved the clockwise sequence would generate imagery with increasing time from left to right.

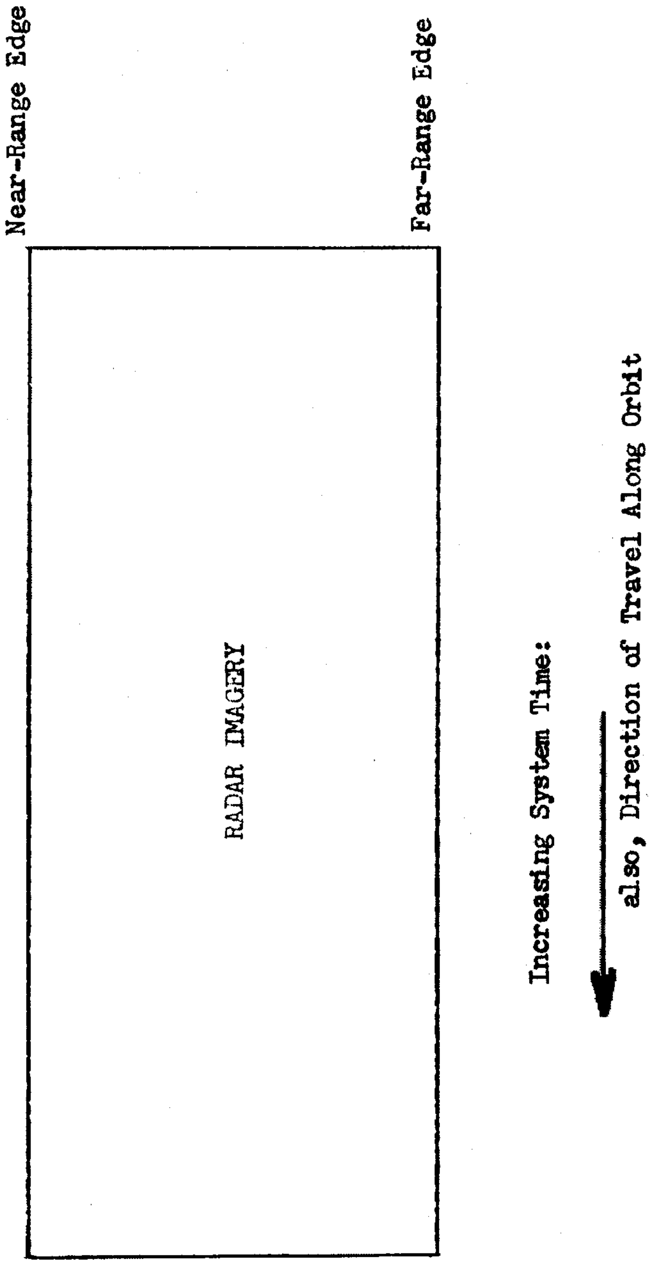

Figure 1.6.0 Image Orientation for Proper Viewing

As had been stated and is evident from the imagery, the aspect ratio of ground-range to azimuth scale factors is not 1:1; instead, the azimuth dimension appears to have been "stretched" by roughly 66 per cent. This is a consequence of the preservation of a 1:1 aspect ratio of slant range to azimuth scale factors at the system depression angle.

Several of the images are accompanied by U.S. Geological Survey Maps bearing an arrow designating true North. The swath between the inner edges of the shaded lines matches the swath imaged by the radar. Each image is also accompanied by a summary of pertinent events and highlights of the imagery itself. The combination of the U.S.G.S. map and the radar imagery constitutes the figure as numbered under the radar image. It is to be recalled that the motion of the satellite is from the right to the left of the radar image-as viewed by the reader.

Figure 1.6.1 Summary

Richmond, Virginia: Pass 14

System Time: 57968.6(ON) - 57973.0(H.V. ON) secs ZT, 22 December 1964

Local Time and Date: 11:06 A.M. EST, 22 December 1964

Local Surface and Weather Conditions:

Ground damp to dry. Overcast, tops of clouds at 2500 to 4500 ft. No frontal activity.

Vehicle Attitude Behavior:

Pitch: Slowly negative-going near center of deadband.

Roll: Holding constant at center of deadband.

Yaw: Has just completed approach to negative edge of deadband, holding constant at edge.

Clutterlock Integrator Behavior (F-60):

On the basis of analog data only, the clutterlock output held roughly constant over this time interval.

RF Signal-to-Noise Ratio (Computed from F-53):

The RF SNR was 14 to 15 db during generation of the image.

PRF Adjustment Status:

The radar prf was 8449 pps during generation of this image (P/L Step 8). On the basis of the image intensity variation with range, it appears that the range gate was being initiated too soon. A lower prf would have led to a more balanced distribution. Some compensation was employed during the optical processing.

Scale Factors of Figure 1.6.1 Print:

Azimuth:	2.09 n.mi/inch
Ground Range:	3.48 n.mi/inch

Highlights of Imagery:

The radar display included most of Richmond, Virginia, and clearly shows the radial transportation network centered on this large city. Many bridges crossing the James River are evident, including one mile-long elevated railway structure nearly parallelling the river inside the city. Very large areas of block and street patterns can be seen. Numerous industrial areas stand out, showing their frequent relationship to transport routes, especially to railroads (generally, thin dark lines are roads, while bright ones are railroads). Outside the city, cultivation, wooded areas, and drainage features can be recognized.


Lorrain
HENRICO

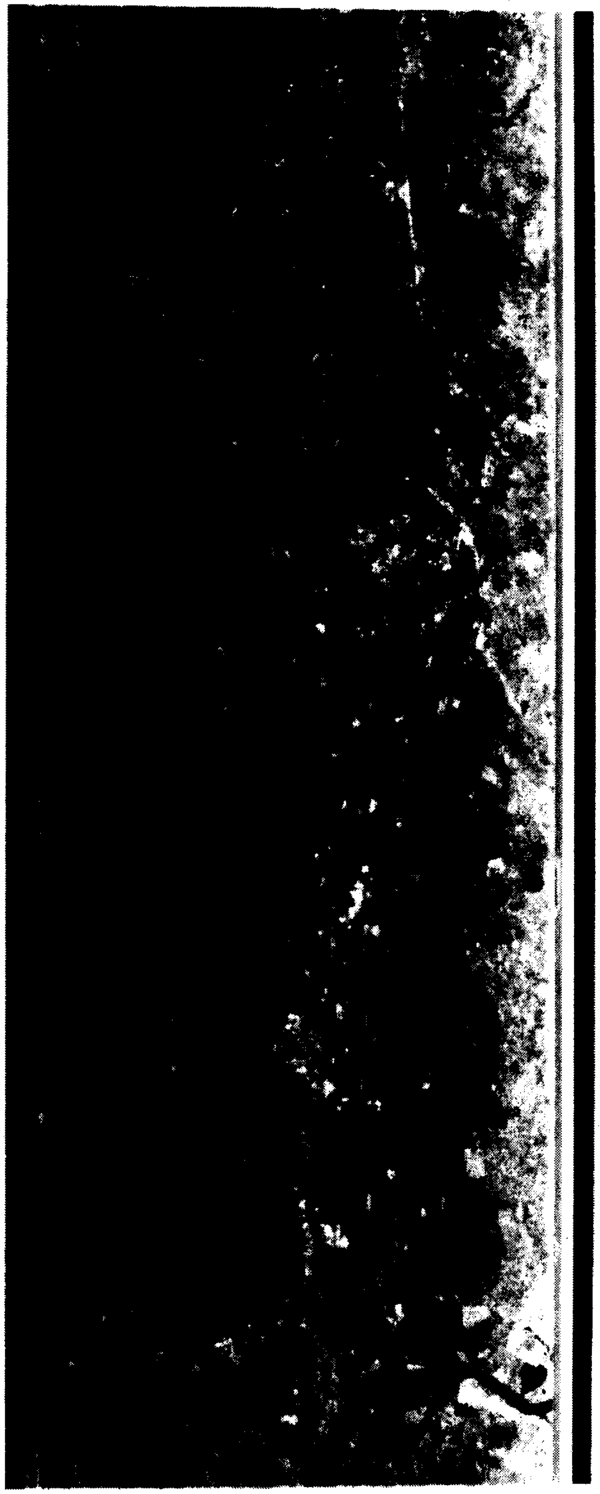

FIGURE 1.6.1 RICHMOND, VIRGINIA; PASS 14

Figure 1.6.2 Summary

Hammond - Chicago; Pass 24

System Time: 23868.7(ON - 23873.0(H.V. ON) secs ZT, 23 December 1964

Local Time and Date: 00:38 A.M. CST, 23 December 1964

Local Surface and Weather Conditions:

Ground wet from rain and fog. Light showers, fog. Winds 10 mph, temperature 39°, dew point 39°. Overcast 200 feet, top at 1500-2000 feet, higher clouds above 8000 ft. Temperature inversion at 2000 feet. No frontal activity.

Vehicle Attitude Behavior:

Pitch: Has just reached negative edge of deadband, holding constant.

Roll: Has just left positive edge of roll deadband, rotating toward center.

Yaw: Holding constant attitude in center of deadband.

Clutterlock Integrator Behavior (F-60):

Some fluctuation in output over time interval of interest

RF Signal-to-Noise Ratio (Computed from F-53):

RF signal-to-noise ratio about 14 db on land, south of industrial area; reaches a local peak of 16 db in industrial complexes, then drops to about 2 db over Lake Michigan.

PRF Adjustment Status:

The radar prf was 8381 pps during generation of this image (P/L step 10). The range gate occurred at a near-optimum time and yielded an image of balanced intensity across the range interval without necessity for compensation in the processor.

Scale Factors of Figure 2 Print:

Azimuth:	2.10 n.mi/inch
Ground Range:	3.48 n.mi/inch

Highlights of Imagery:

Because of the high density of strong targets in the industrial areas, as well as the effect of the shoreline on the automatically controlled gain, two different processing exposures are presented. The stronger exposure shows better "ground-painting", while a lesser exposure improves the appearance of the concentration of bright returns. The shoreline and waterfront features are easily recognized. The apparently man-made harbor at the short-range (top) edge of the swath shows construction changes made since the map was up-dated. Some of the railroad routes show as low-return lines through heavily built-up surroundings; most appear as bright-line returns. As the shoreline gradually crosses the swath, the continually increasing gain tends to over-expose the small remaining land area.

A close inspection of the output transparencies recorded at the two different exposure levels would show that the exposure which provides adequate ground painting has degraded resolution in the strong-target complex. This degradation occurs at the output recording stage, partly as a consequence of "blooming" of bright fine resolution images unless special fine-grain but slow emulsions are employed, and partly as a result of the point-target sidelobes being sufficiently intense to reach the saturation level of film. The fact that the large dynamic range associated with the reflectivity of a scene including both agricultural terrain and an industrial complex exceeds the dynamic range of some of the system elements, is illustrated by this sample of imagery.

AC-04306

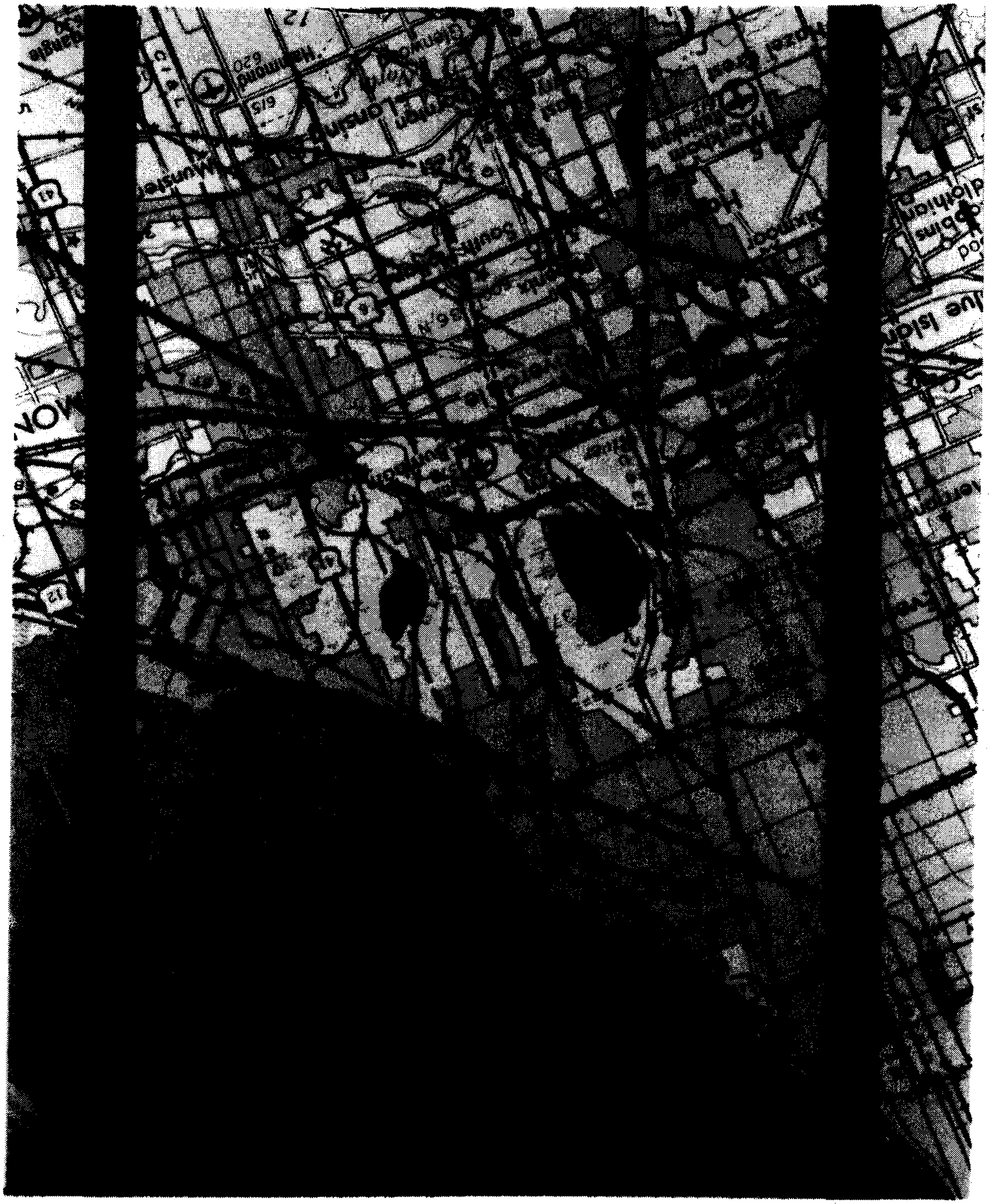

[redacted]

[redacted]

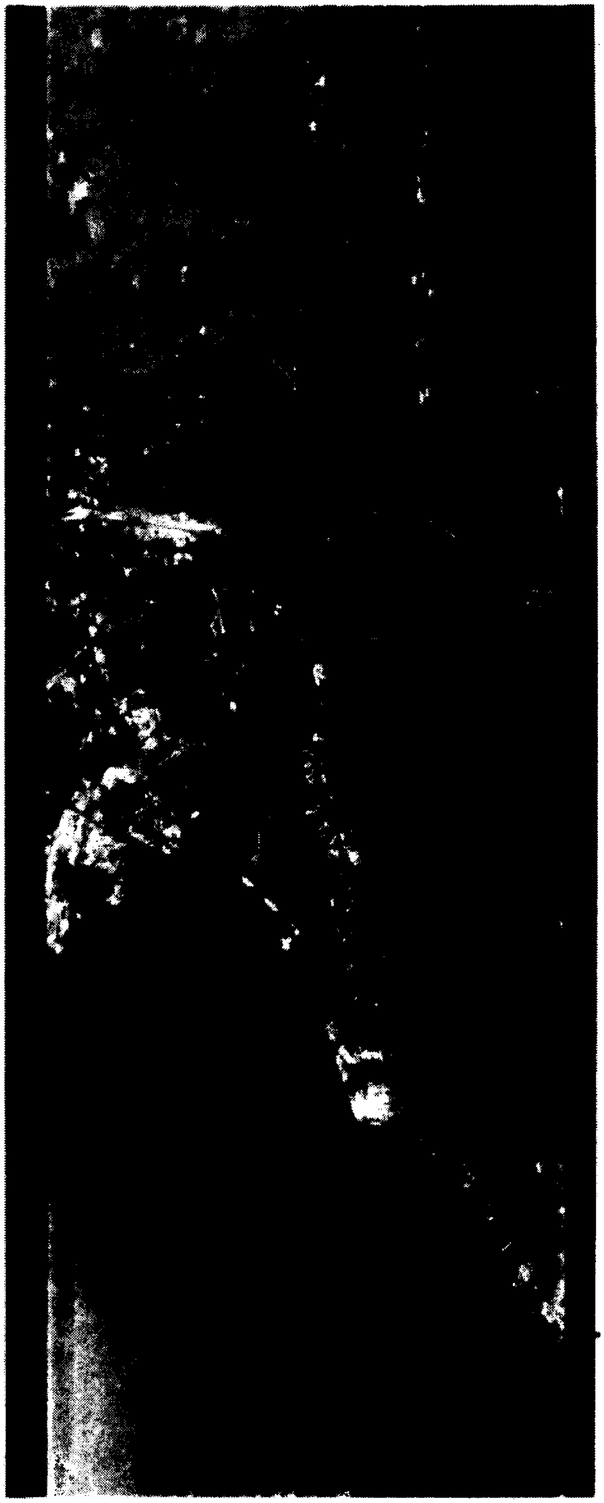

Figure 1.6.2(a) - Hammond, Indiana - Chicago, Illinois - Processor Output Film - Exposure Fitted to Natural - Terrain Returns.

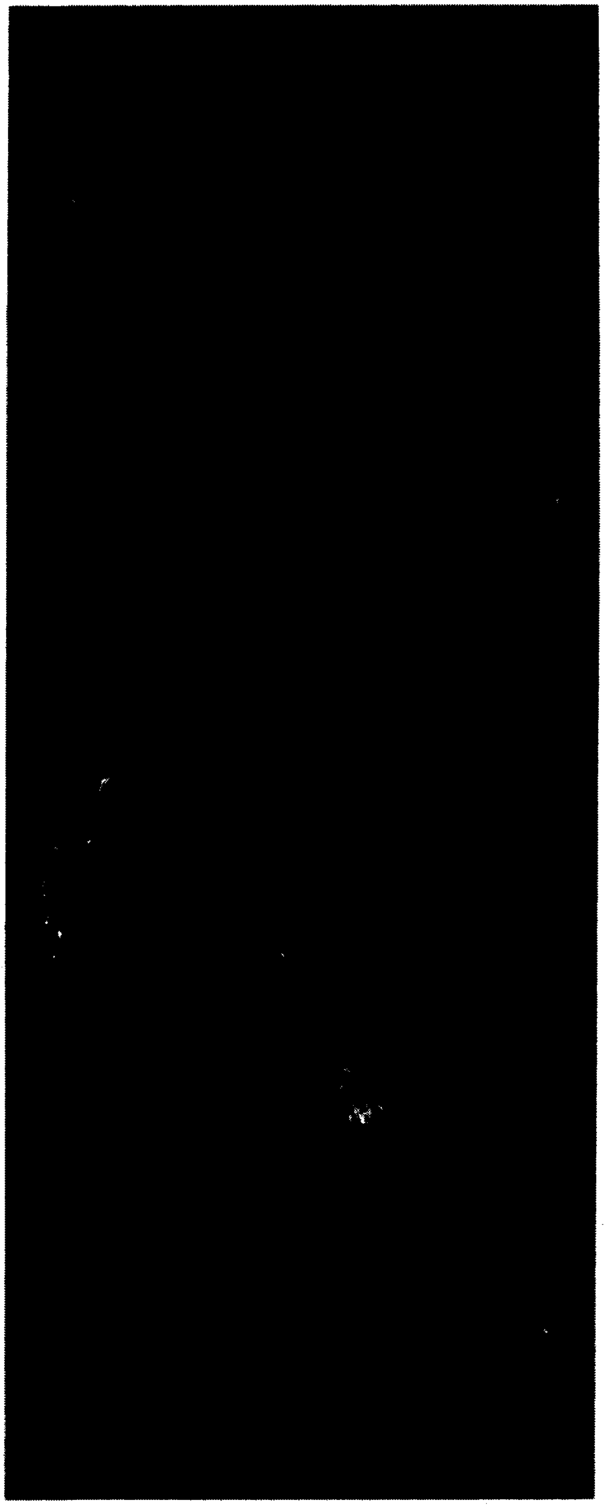

Figure 1.6.2(b) - Hammond, Indiana - Chicago, Illinois - Processor Output Film - Exposure Fitted to Strong Culture Returns.

Figure 1.6.3 Summary

Wurtsmith Air Force Base, Michigan: Pass 30

System Time: 57421.8 (ON) - 57426.2 (H.V. ON) secs ZT, 23 December 1964.

Local Time and Date: 10:57 A.M. EST, 23 December 1964.

Local Surface and Weather Conditions:

Snow cover on ground, depth variable, in excess of two inches. Fog; sky obscured. Wind conditions -- calm. Visibility, one mile. Stationary front present. Cloud tops at 9-10,000 feet.

Vehicle Attitude Behavior:

Pitch: Holding constant at positive edge of deadband.

Roll: Had been holding constant 0.1° on negative side of deadband center; slowly rotating positively, toward center.

Yaw: Rotating at rate of .005 deg/sec toward positive edge of deadband, already past deadband center by about 0.1°.

Clutterlock Integrator Behavior (F-60):

Turn-on transient had settled out; gradual negative-going trend in process, local reversal occurs during generation of this image.

RF Signal-to-Noise Ratio (Computed from F-53):

RF signal-to-noise ratio has a maximum value of 14 db over land mass, dropping to 1 db for the over-water portion.

NRO APPROVED FOR RELEASE
DECLASSIFIED BY: C/IART
DECLASSIFIED ON: 9 JULY 2012

PRF Adjustment Status:

The radar prf was 8449 pps during generation of this image (P/L step 8). Range gate occurred at optimum time and map intensity is well balanced without need for compensation in the processor.

Scale Factors of Figure 3 Print:

Azimuth:	2.09 n.mi/inch
Ground Range:	3.48 n.mi/inch

Highlights of Imagery:

This SAC facility stands out unmistakably from its wooded surroundings between Michigan's Lake Huron shore and the Au Sable River. Many roads, including some little-traveled ones, are seen as narrow gaps in the tree cover, although some such gaps are power-line clearings. Two large areas of cleared land show where the forest has given way to farmland, the outlines of many individual clearings correlating very closely with the outlines shown by shading on the map. Two dams and the reservoirs they form are readily detected and identified. (The power distribution lines from the hydroelectric plants are not evident against this high-return background; they have been found emanating from some other plants seen by this system in more open country. An example of a steel-tower line can be seen in Figure 1.6.5.) Some along-shore ice masks the true shore-line of Lake Huron, especially in Tawas Bay. The automatic gain control effect is very pronounced in the region of Tawas Point.

Aerial Photographs

Figures 6-35a and 6-35b are aerial photographs of Wurtsmith Air Force Base, taken from a B-52 aircraft (Blackbird Project), on 11 March 1965, at an altitude of 40,500 feet MSL. The camera utilized was an aerial T-11, f6.3, frame camera with 6 inch focal length. Shutter speed was 1/500 second. The camera resolution is approximately 50 lines/millimeter. Figure 1.6.3(a) is photographically reduced from the camera negative image size, to a scale factor which closely approximates the radar image given in Figure 1.6.3. Figure 1.6.3(b) is a 2:1 enlargement of the aircraft camera negative. This SAC air base can be seen to contain four (4) aircraft on the parking ramp (runway side), in the six parking areas, in a similar parking arrangement to that observed by the satellite radar. Further study of the two imaging methods reveal the complementary nature of radar imagery, to that of photography.

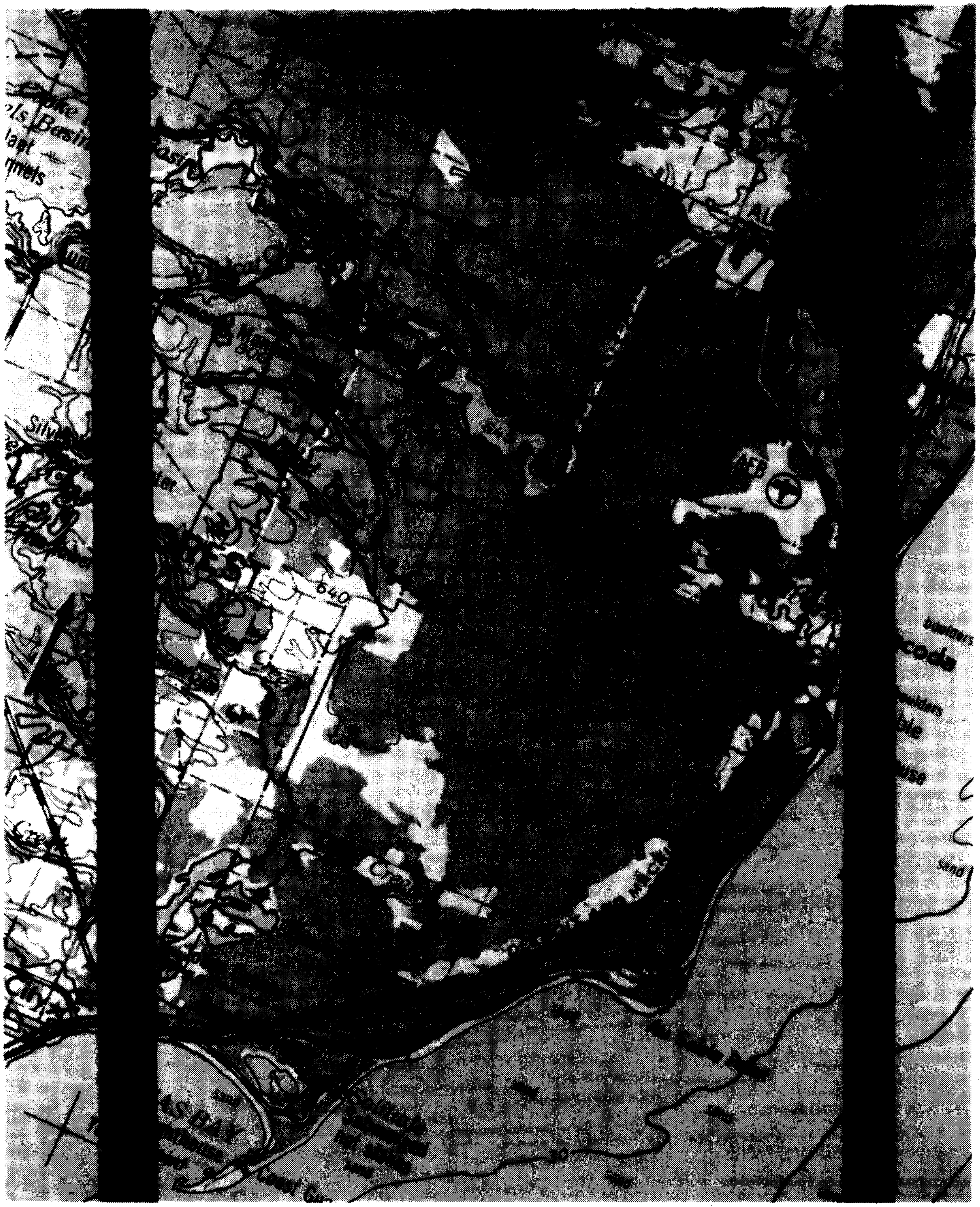
640
AFB

FIGURE 1.6.3 WURTSMITH AFB, MICHIGAN; PASS 30

FIGURE 1.6.3 (a) B-52 Aerial Wurtsmith AFB 11 March 1965

FIGURE 1.6.3 (b) B-52 Aerial Wurtsmith AFB 11 March 1965

Figure 1.6.4 Summary

Ohio Turnpike Crossing; Pass 30

System Time: 57473.5(ON) - 57478.0(H.V. ON) secs ZT, 23 December 1964

Local Time and Date: 10:58 A.M. EST, 23 December 1964

Local Surface Weather Conditions:

Ground wet from recent rain. Light rain showers in progress, fog. Winds at 10 knots. Visibility one mile. Overcast at 500 to 1000 feet. Cloud tops at 9 - 10,000 feet.

Vehicle Attitude Behavior:

Pitch:	Holding constant, somewhat positive with respect to deadband center.
Roll:	Slowly rolling toward positive side, about in center of deadband.
Yaw:	Had reached positive edge of limit cycle shortly before, now slowly negative-going away from positive edge.

Clutterlock Integrator Behavior (F-60):

Holding roughly constant with some fluctuation in output.

RF Signal-to-Noise Ratio (Computed from F-53):

RF signal-to-noise ratio about 15 to 16 db.

PRF Adjustment Status:

The radar prf was 8449 pps during generation of this image (P/L step 8). Range gate occurred at optimum time; image intensity therefore constant across range interval, and no compensation in the processor was necessary.

Scale Factors of Figure 4 Print:

Azimuth:	2.09 n.mi/inch
Ground Range:	3.48 n.mi/inch

Highlights of Imagery:

The display shows the division of this highway into east-bound and westbound lanes. The actual separation is sometimes very large, and the inter-lane return can be seen with the naked eye. But even where the division lessens, use of a magnifier will show that there is paired structure along nearly all of the displayed portion of the turnpike. The complex structure of the valley of the Cuyahoga River is shown by shadings which are probably due to vegetation variations as much as to slopes. Other highways, railroads, cultivation patterns, and small lakes are recognizable. The outskirts of Cleveland reach into the right-hand end of the display.


1250
1250

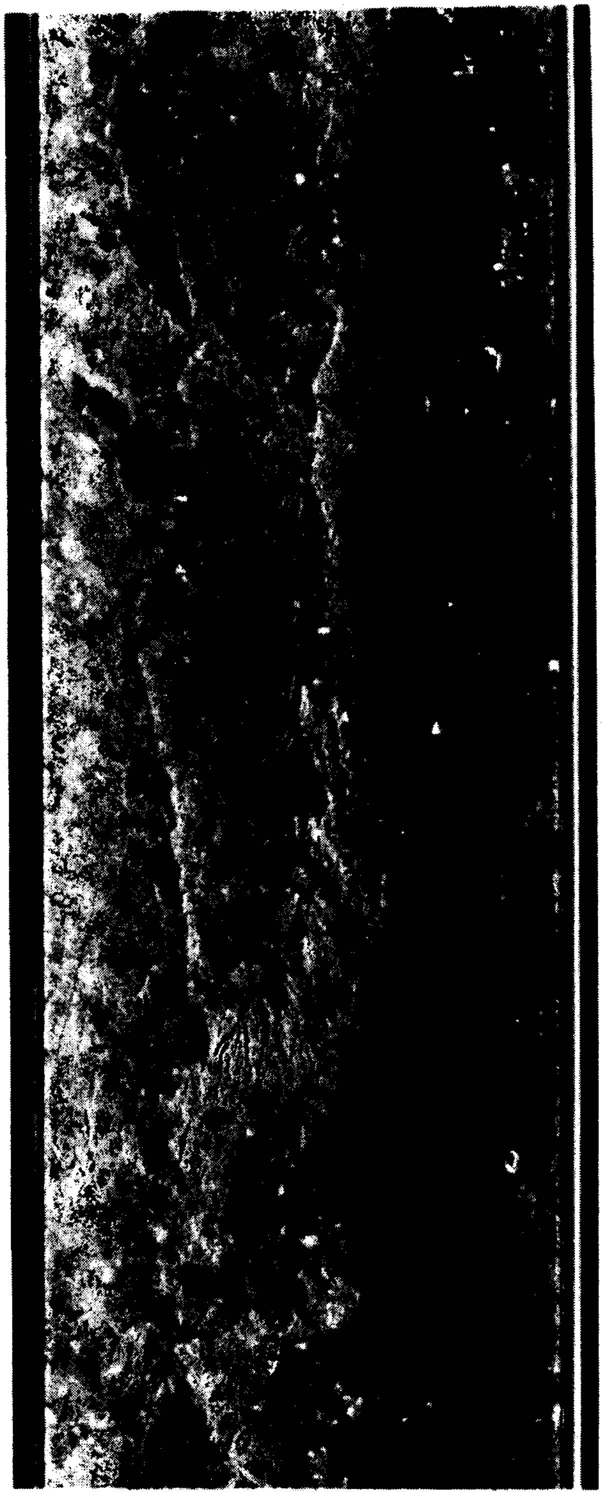

FIGURE 1.6.4 OHIO TURNPIKE CROSSING: PASS 30

Figure 1.6.5 Summary

Ligonier, Indiana: Pass 8

System Time: 24295.0(ON) - 24299.3(H.V. ON) secs ZT, 22 December 1964

Local Time and Date: 1:45 A.M. EST, 22 December 1964

Local Surface and Weather Conditions:

Ground wet, melted snow and ice. Light fog, visibility 2-3 miles, temperature 30°, dew point 29°F. Overcast, ceiling few hundred feet. No important frontal activity. Temperature inversion at 2500 feet.

Vehicle Attitude Behavior:

Pitch: Constant, to positive side of deadband center.

Roll: Constant, slightly to negative side of deadband center.

Yaw: Undergoing positive yaw, toward positive side of deadband center but not yet at edge of limit cycle.

Clutterlock Integrator Behavior (F-60):

VCO output frequency decreasing rapidly with jagged reversal in vicinity of region shown.

RF Signal-to-Noise Ratio (Computed from F-53):

RF SNR about 10 db.

PRF Adjustment Status:

The radar prf was 8314 pps during generation of this image (P/L step 12). Range gate was occurring too late with respect to video arrival; an increase in prf was required, to reduce interpulse time and provide a better time coincidence. Some compensation was provided in the optical processor.

Scale Factors of Figure 1.6.5 Print:

Azimuth:	2.10 n.mi/inch
Ground Range	3.48 n.mi/inch

Highlights of Imagery:

This display segment was selected because it contains two indications of moving railway traffic. Because this type of radar infers positions of objects from their average doppler frequencies, moving objects are seen at their proper ranges, but misplaced parallel to the satellite track by amounts dependent on each object's motion. Thus, from the radar system data alone, we determine that the short bright-line return between Lake Wawasee (at lower edge of display) and the B & O Railroad tracks just to the left of the lake represents a train 3200 feet long (hence about 65 cars) which was westbound at 38 mph at 01:44:56.4 AM EST. A 36 mph eastbound train of about 85 cars (and perhaps more) appears to the left of NYC tracks near the upper edge of the display; this train was observed 1.6 seconds after the first.

The line of bright dots running vertically just right of Ligonier is part of an electric power transmission line, each dot being one steel tower. The returns within Lake Wawasee represent ice. The strong returns in the small towns located on railroads are characteristic; similar towns served only by roads generally lack these stronger returns. While most of the Elkhart River is too narrow to be seen as a watercourse, its route is easily traced by the band of uncut vegetation that borders it through the surrounding farmland.


ELKH.
LAGRANGE

AC-04306

FIGURE 1.6.5 LIGONIER, INDIANA: PASS 8

Figure 1.6.6 Summary

Canyon and Mesa Terrain: Pass 9

System Time: 29556.3(ON)- 29560.6(H.V. ON) secs ZT, 22 December 1964

Local Time and Date: 1:13 A.M. MST, 22 December 1964

Local Surface and Weather Conditions:

Clear, temperature 46° F, dew point 43°, visibility 15 miles. No frontal activity, winds 5 mph or less, area in high pressure region. Surface dry.

Vehicle Attitude Behavior

Pitch: Holding at positive edge of deadband.

Roll: Attitude had been slightly to positive side of center, now settling across center.

Yaw: Had been yawing negatively, about to hit negative edge of deadband.

Clutterlock Integrator Behavior (F-60):

VCO reaching local maximum in frequency, some wandering.

RF Signal-to-Noise Ratio (Computed from F-53):

R F signal-to-noise ratio ranged from 11 to 14 db.

PRF Adjustment Status:

The radar prf was 8381 pps during generation of this image (P/L step 10). Range gate was occurring slightly too early and adjustment to a slightly lower prf was in order; the uneven illumination across the swath was partially compensated during the optical processing.

Scale Factors of Figure 6 Print:

Azimuth:	2.10 n.mi/inch
Ground Range:	3.48 n.mi/inch

Highlights of Imagery:

These canyons which cut into a relatively flat plateau are located about 80 miles north and 20 miles east of Phoenix, Arizona. The importance of viewing radar imagery with the radar's near-range upward can be seen by rotating this page 180°, putting far-range upward. (Also compare the isolated mountain ridges shown in Figure 1.6.11.) The map shadings representing forestation are not matched by tones on the display. This contrasts with the clearly identifiable shapes of woodlots and clearings that are seen in Midwestern areas (for example, Figure 1.6.3).

AC-04306


YAVAPAI COUNTY
COCONINO COUNTY
Mud Tank Draw
Cabin
Y Lazy Y Ranch
13 MILE ROCK
Ranger Station
BALD HILL
6770
Creek
WALKER MOUNTAIN
Walker
COCONINO NATIO
6515
6917
5555
4750

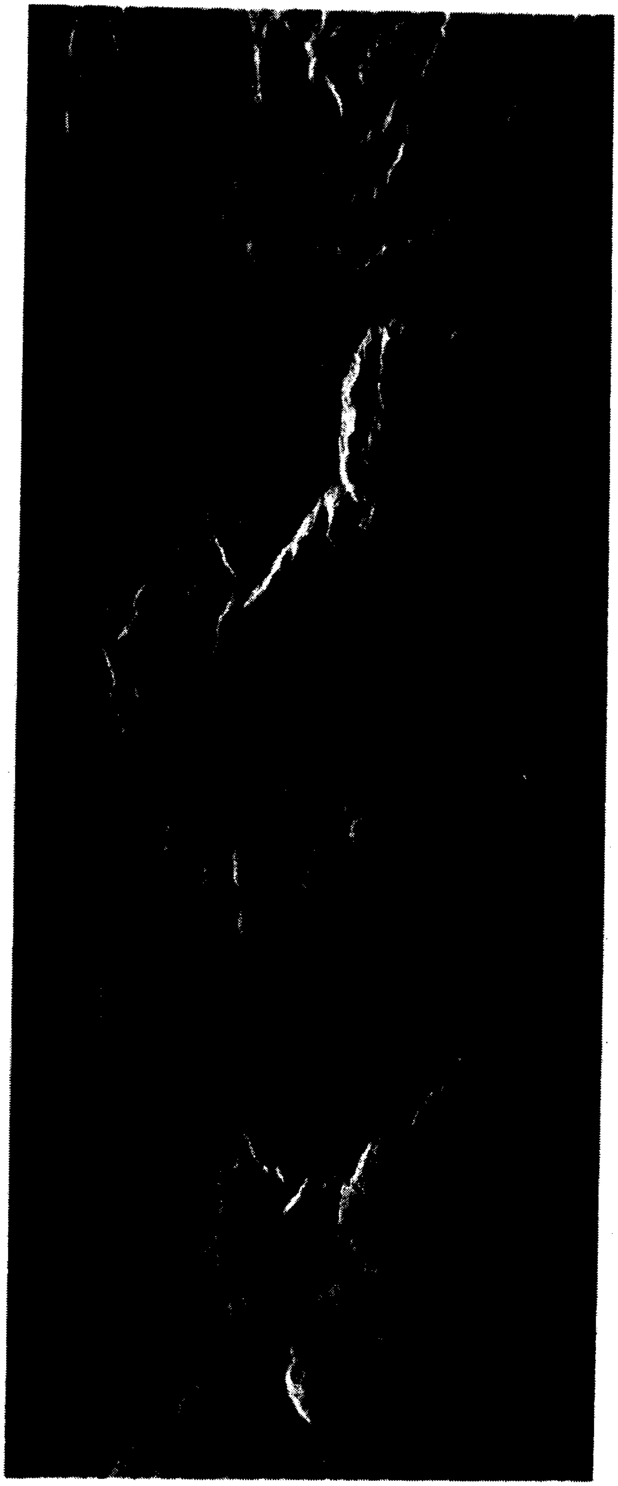

FIGURE 1.6.6 CANYON AND MESA TERRAIN: PASS 9

Figure 1.6.7 Summary

Mountainous Terrain: Pass 25

System Time: 29213.0(ON) - 29217.3(H.V. ON) secs ZT, 23 December 1964

Local Time and Date: 01:07 A.M. MST, 23 December 1964

Local Surface and Weather Conditions:

Ground dry, some snow on mountain tops. No precipitation; winds from south at 20 mph, gusts to 30 mph. Temperature about 55°F, dewpoint 22°F. Near northern edge of high pressure area. Overcast 8500 feet, scattered clouds at 6000 feet. Clouds extending to 20,000 feet, contained ice and turbulence.

Vehicle Attitude Behavior:

Pitch: Holding constant pitch attitude at positive edge of deadband.

Roll: At center of deadband, slowly rolling toward negative side.

Yaw: Holding constant yaw attitude at center of deadband.

Clutterlock Integrator Behavior (F-60):

Wandering slowly about constant value.

R F Signal-to-Noise Ratio (Computed from F-53):

R F signal-to-noise ratio ranges from 13 to 15 db.

PRF Adjustment Status:

The radar prf was 8415 pps during generation of the above image (F/L step 9); this was an optimum position, for which the range gate coincided with the returning video.

Scale Factors for Figure 1.6.7

Azimuth:	2.10 n.mi/inch
Ground Range:	3.48 n.mi/inch

Highlights of Imagery:

The area shown lies midway between Provo and Price, Utah. The pass running across the display contains a stream, a highway, and a railroad. The railroad is visible nearly all the way, including its hairpin turn. The smooth-textured area at the upper right is a reservoir bordered by a railroad. Splotchy texture on mountains may be irregular forestation, or may be related to snow cover. Shadings on plateau at lower left correlate fairly well with forestation shadings on map.

The elevation variation of from 7200' to over 9000' results in range-direction relief displacements that vary by 0.5 n.mi., or 0.2 inch at the scale of the map reproduction above. That is, if an along-track line on the display (such as a swath-edge line) were to be transformed accurately to its corresponding location on the map, it would deviate from straightness by that much. (The largest amount of distortion of the range scale found to date in any of the imagery generated during this test is 1.2 n.mi. or, at the scale of the map reproduction, 0.6 inch.)

AC-04306

FIGURE 1.6.7 MOUNTAINOUS TERRAIN: PASS 25

Figure 1.6.8 Summary

Eel River, California   Pass 16

System Time: 68664.7(ON) - 68669.0(H.V. ON) ZT, 22 December 1964

Local Time and Date: 11:04 A.M. PST, 22 December 1964

Local Surface and Weather Conditions:

Entire area wet, rain for several previous days. Flood conditions present. Rain, occasionally heavy. Winds from 180° at 10 knots. Scattered cloud layer 700-1000 feet, overcast at 1400-2500 feet. Low pressure area.

Vehicle Attitude Behavior:

Pitch: Holding constant at positive edge of deadband.

Roll: Wandering slowly on negative side of deadband center.

Yaw: At center of deadband, in process of yawing toward positive edge at rate of 0.015 deg/sec.

Clutterlock Integrator Behavior (F-60):

Oscillator changing frequency in negative direction, apparently still heading toward correct output for initial attitude at turn-on.

R F Signal-to-Noise Ratio (Computed from F-53):

R F signal-to-noise ratio about 8 db over water, in process of rapidly increasing to 15 db in region where land occupies full swath width. Water reflectivity rather high due to noticeable wave structure.

PRF Adjustment Status:

The radar prf was 8381 pps during generation of this image (P/L step 10). The range-gate occurrence was not properly synchronized with the returning video--the former was too early. A reduction in prf and consequent increase in inter-pulse time would have led to a better coincidence. The poor image intensity distribution was partially compensated in the optical processor.

Scale Factors of Figure 1.6.8 Print:

Azimuth:	2.09 n.mi/inch
Ground Range:	3.48 n.mi/inch

Highlights of Imagery:

The disastrous floods that occurred in northern Pacific Coastal areas just before Christmas of 1964 were sampled by some of the imagery generated during this mission. In the example shown, the flood plain around the mouth of the Eel River is largely under water. Only occasional portions of the lowlands show above the water. The thin-line returns mostly border streams, hence are probably vegetation projecting above the flood waters. One short, straight, very bright return suggests a bridge whose approach roads are not visible. The streaked pattern on the flood waters suggests areas of wind-caused waves with quieter surface in the lee of obstructions; if so, the wind direction within this small area was SW instead of S.

Wave structure is clearly seen on the ocean, with altered wave forms close to shore. The effect of the escaping river current can be seen over a 90° arc nearly 10 n.mi. long and extending 5.5 n.mi. offshore. The major escape channel is not at the normal river mouth, but via a break in the coastal barrier nearly a mile farther up the coast.


sand
mud
Table Bluff Lighthouse
Cannibal Island
Hawley Island
EEL RIVER
Salt River
Island School
Grant Union School
Port Kenyon
Arlynda Corners
Ferndale
Waddington
Bluff
10
6
30
50

Pages 6-57, 6-58, 6-59, and 6-60 are missing

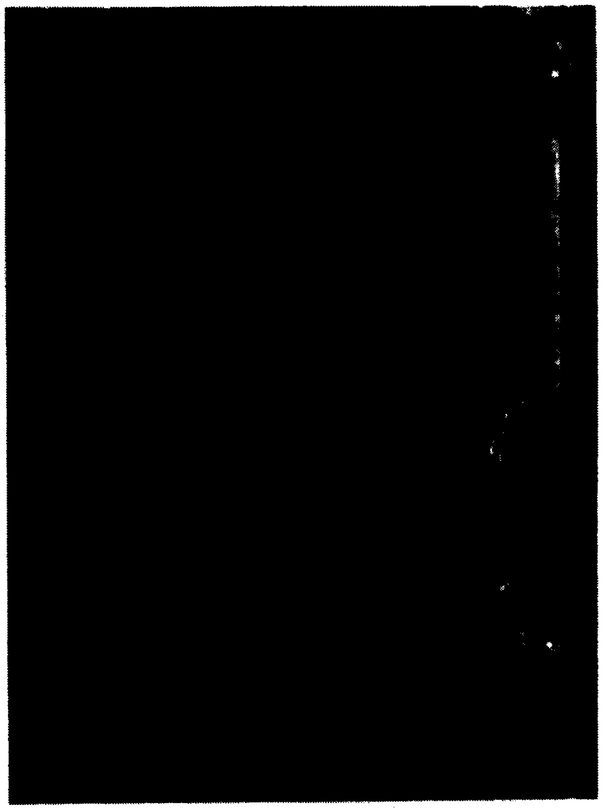

FIGURE 1.6.9(a) MOTHBALL FLEET NEAR WILMINGTON, NORTH CAROLINA: PASS 30

AC-04306

FIGURE 1.6.9(b) CLOSEUP OF MOTHBALL FLEET

Figure 1.6.10 Summary

Ships in Pacific: Pass 16

System Time: Ships at 68713.1 and 68717.3 ZT, 22 December 1964

Local Time and Date: 11:05 A.M. PST, 22 December 1964

Local Surface and Weather Conditions:

Scattered heavy rain, winds from 200° at 26 to 30 knots. Scattered cloud layer at 700-1000 feet, overcast at 1400-2500 feet. Layered clouds with tops at 35,000 feet.

Vehicle Attitude Behavior:

Pitch: Holding constant at positive edge of deadband.

Roll: Holding constant at positive edge of deadband.

Yaw: Vehicle starting to return slowly from positive edge of deadband.

Clutterlock Integrator Behavior (F-60):

Oscillator output fluctuating slightly about a relatively steady value.

RF Signal-to-Noise Ratio (Computed from F-53):

The RF signal-to-noise ratio due to the water return in the vicinity of the ships ranged from 7 to 8 db. Measurements of the returning power level were taken at the rate of one sample every 1.2 to 1.3 seconds, and none of the samples in this time interval showed a significant increase in return power due to the vessels themselves. The duration of each sampling period was about 0.017 seconds.

PRF Adjustment Status:

The radar prf was 8381 pps during generation of this image (P/L step 10). The range-gate occurrence was not properly synchronized with the returning video--the former was too early. A reduction in prf and consequent increase in interpulse time would have led to a better coincidence. The poor image intensity distribution was partially compensated in the optical processor.

Scale Factors of Figure 1.6.10 Prints:

Figures 1.6.10(a) and 1.6.10(c)

Azimuth:	2.09 n.mi/inch
Ground Range:	3.48 n.mi/inch

Figures 1.6.10 (b) and 1.6.10(d)

Azimuth:	100 ft/mm
Ground Range:	166 ft/mm

Highlights of Imagery:

Ships were seen by the system on the Pacific, Atlantic, Great Lakes, and some inland rivers. The two shown as examples were spotted off the California coast, during the fourth mapping pass. The one seen first, and giving the smaller return, was 20 n.mi. off the Golden Gate, between the lightship and the Farallon Islands; specifically, at 37.74°N, 122.90°W. The return is 700 to 800 feet long and is aligned at 151° - 331° azimuth (true). However, since any rotational motions (e.g., roll) of a vessel would produce doppler effects tending to spread the processed returns in the along-track direction, the alignment of the return may not indicate ship heading, nor need the length of the return directly indicate the vessel's size. A faint suggestion of a wake at the northern end of the ship return implies a heading azimuth of 137° true. The second ship was seen at 37.74°N, 122.78°W, or 14 n.mi. west of Half-Moon Bay, 18 n.mi. farther down the coast. The low-return streak to the right is not a wake, but an artifact of the radar's signal-recording process, in which the strong signal from the ship commandeers the available dynamic range of the film opacity, suppressing the adjacent faint signals. Similar adjacent-signal suppression can be seen near the bottom of Figure 1.6.11.

[redacted]

FIGURE 1.6.10(a) FIRST SHIP IN PACIFIC

FIGURE 1.6.10(b) CLOSEUP OF FIRST SHIP

AC-04306

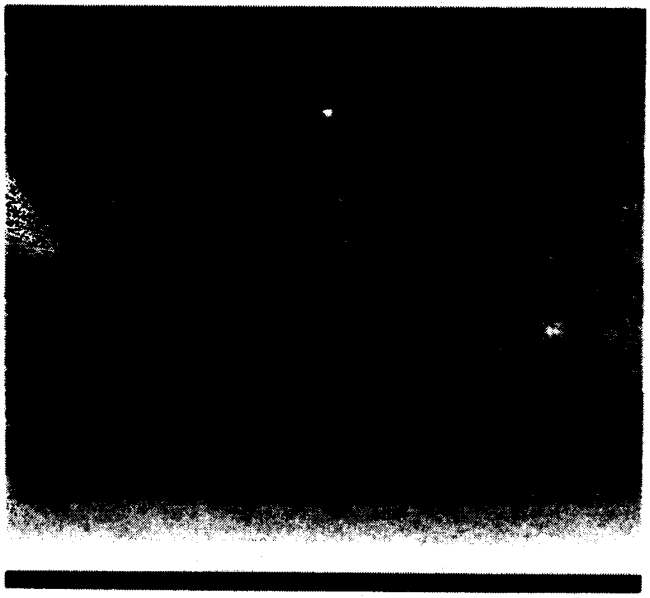

FIGURE 1.6.10(c) SECOND SHIP IN PACIFIC

FIGURE 1.6.10(d) CLOSEUP OF SECOND SHIP

NRO APPROVED FOR RELEASE
DECLASSIFIED BY: C/IART
DECLASSIFIED ON: 9 JULY 2012

Figure 1.6.11 Summary

Phoenix, Arizona: Pass 9

System Time: 29537.8(ON) - 29542.2(H.V. ON) ZT, 22 December 1964

Local Time and Date: 1:12 A.M. MST, 22 December 1964

Local Surface and Weather Conditions:

Clear, temperature 46°F, dew point 43°, visibility 15 miles. No frontal activity, winds 5 mph or less, area in high pressure region. Surface dry.

Vehicle Attitude Behavior:

Pitch: Had just completed positive-going swing, now holding at edge of limit cycle.

Roll: Slightly to positive side of zero, slowly returning to center of deadband.

Yaw: Undergoing negative-going yaw, about in center of deadband.

Clutterlock Integrator Behavior (F60):

VCO frequency output increasing roughly linearly, at slightly under 0.1 Kc/sec. No jagged behavior.

RF Signal-to-Noise Ratio (Computed from F-53)

R F signal-to-noise ratio ranged from 11 to 13 db.

PRF Adjustment Status:

The radar prf was 8381 pps during generation of this image (P/L step 10). The range gate occurred too early with respect to the returning video; a change to a reduced prf, hence increased interpulse time, was required. The imbalance in image intensity was partially compensated in the optical processor.

Scale Factors of Figure 1.6.11 Print:

Azimuth:	2.10 n.mi/inch
Ground Range:	3.48 n.mi/inch

Highlights of Imagery:

The second time the orbiting system was turned on, it promptly caught Phoenix, Arizona, practically centered in the swath, the display being filled by this extensive metropolitan area. Obvious features in the display are the two ranges of mountains that constrict the city to North and South, the wide bed of the Gila River crossing the southern half of the city, and the cultivated rural area fringing it on the west. The large dark block at the top of the display is Sky Harbor Airport. The most obvious traffic route is the express highway which leaves the southwest corner of the airport, parallels the river to mid-range, then proceeds due north except for two westward jogs of a few thousand feet each. The railroad along the northern edge of Sky Harbor can be traced across the swath by the associated industrial construction, which gives brilliant radar returns. The diagonal going to the northwest consists of more railroads and the associated facilities. The paralleling major highway (to Los Angeles) can also be seen, especially where it leaves the railroad and continues to slice through the city block structure to east-west Van Buren Street. The curving routes of the Grand Canal and the Arizona Canal can be traced over most of their lengths.


PHOENIX
Tempe
Laveen
SOUTHERN PACIFIC
Sky Harbor
Alhambra
Canal
1087
1063
995
1010
1141
1207
1975
89
80

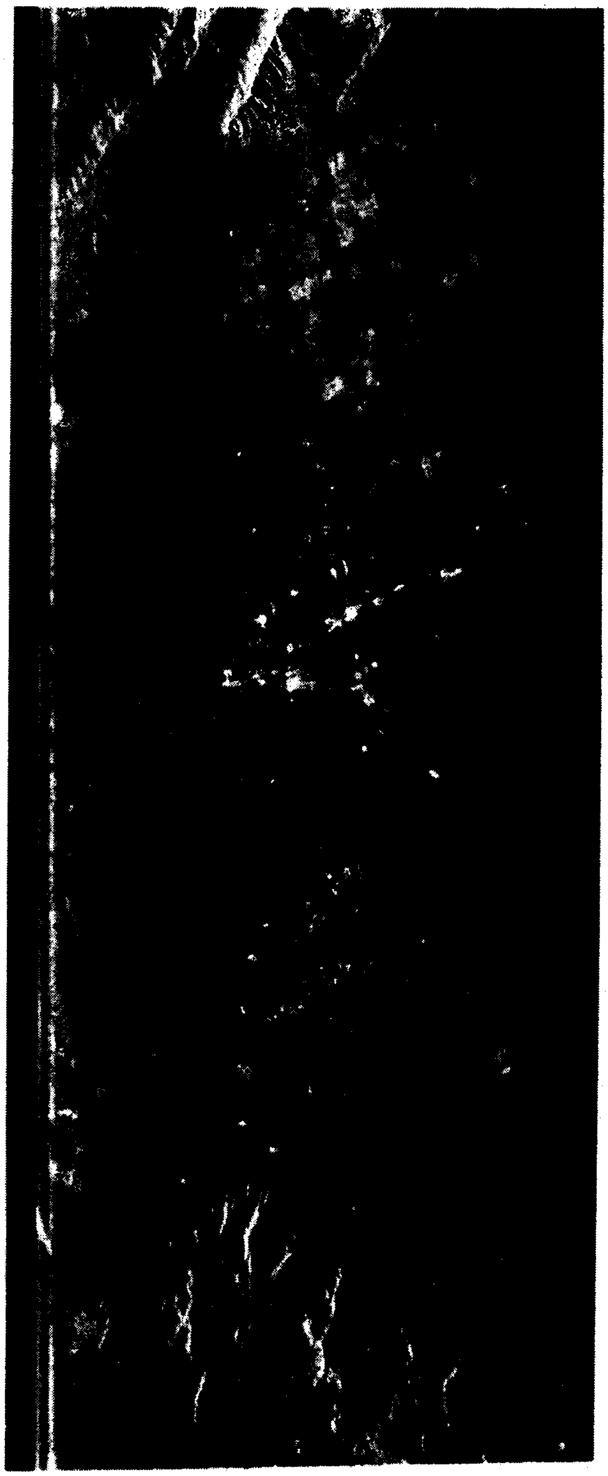

FIGURE 1.6.11 PHOENIX, ARIZONA: PASS 9

Effects of the Data Link and the AMIE Recorder

The video collected via the Wide Band Data Link can be expected to produce radar imagery which is somewhat degraded in range resolution and in dynamic range with respect to the imagery generated from the physically-recovered data. The video stored on the AMIE recorder will be more severely degraded, and will therefore yield radar imagery which is still poorer. The range resolutions which are realized from the Data Link and the Data Link/AMIE data are determined by the effective video bandwidths of the devices, and these values are independent of the location of the satellite with respect to the controlling tracking station. Dynamic range, on the other hand, is dependent upon the video signal-to-noise ratio of the data link, and this varies with the satellite elevation angle and slant range from the station.

An estimate of the azimuth-and range-resolution capabilities of the system in all three modes was made by examining the imagery of the corner reflector array viewed on Pass No. 8. The results are as follows:

Physically Recovered Data

Azimuth Resolution:	10 to 15 feet
Ground Range Resolution:	75 feet

Data-Link Video Data

Azimuth Resolution:	10 to 15 feet
Ground Range Resolution:	100 to 150 feet

Data Link/AMIE Stored Video

Azimuth Resolution:	10 to 15 feet
Ground Range Resolution:	About 200 feet

We note that azimuth resolution is not degraded, but that range resolution is somewhat degraded by the data link characteristics and still further degraded by the effective bandpass characteristic of the AMIE recorder.

For the purpose of making a three-way comparison, the imagery of Phoenix derived from the three video sources has been selected. Figure 1.6.11 above showed the result of processing the physically-covered data. Figure 1.6.12 shows the corresponding image, its generation being identical to that of Figure 1.6.11 with the exception of the use of the Data Link video. Figure 1.6.13 was similarly generated from the data link video stored on the AMIE. The degradation of range resolution from 1.6.11 to 1.6.12 is not immediately apparent because the limiting resolution of the paper print itself masks the difference, which is evident on original output transparencies. The additional degradation due to the AMIE is discernible to the eye.

The imagery of Figures 1.6.11 to 1.6.13 shows a reduction in dynamic range as we progress from Recovery to Data Link

AMIE video. The photographic recorders used in the vehicle and in the ground stations had dynamic ranges of the order of 20 db. At the system time under consideration, the elevation angle of the vehicle with respect to VTS was 10 degrees, and the dynamic range of the data link, as limited by its signal-to-noise ratio, was of the order of 20 to 23 db. The dynamic range of the cascaded data link and recorder was about 17 db. It is evident from the marked degradation of image quality from Figure 1.6.12 to 1.6.13 that the AMIE dynamic range was poor by comparison with this latter value.

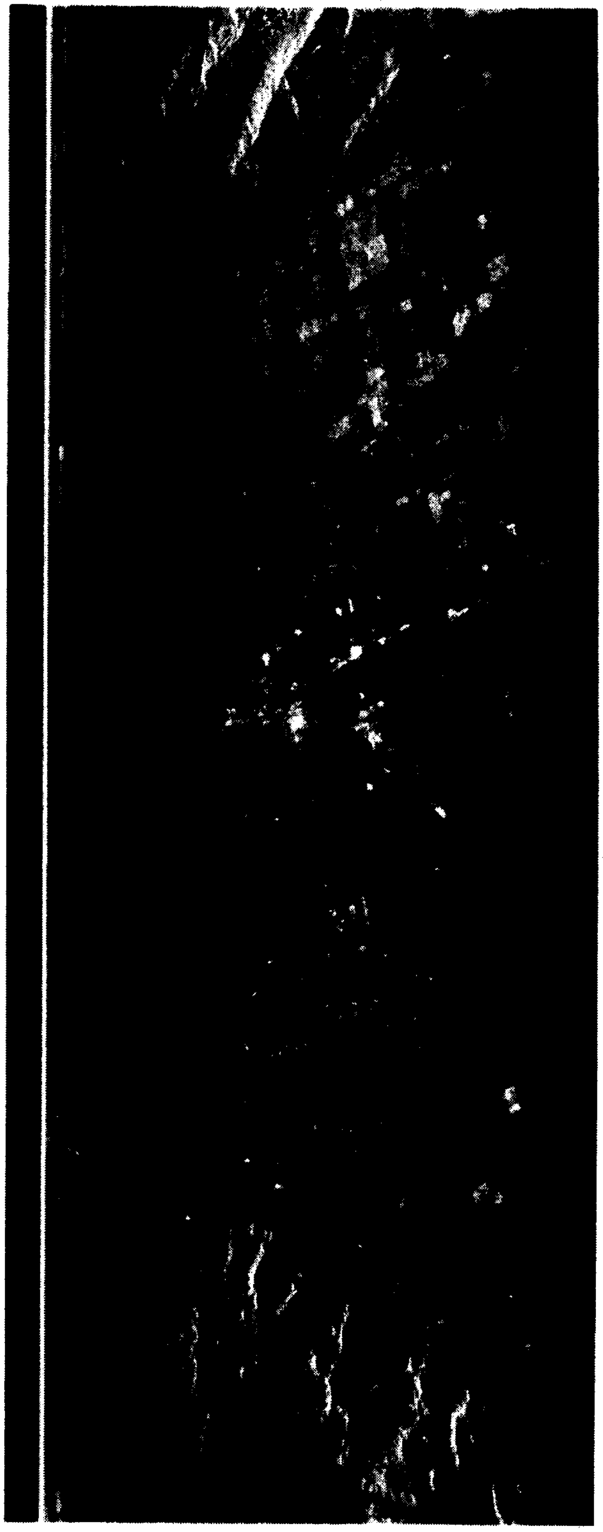

FIGURE 1.6.12 RADAR IMAGE OF PHOENIX GENERATED FROM DATA LINK VIDEO

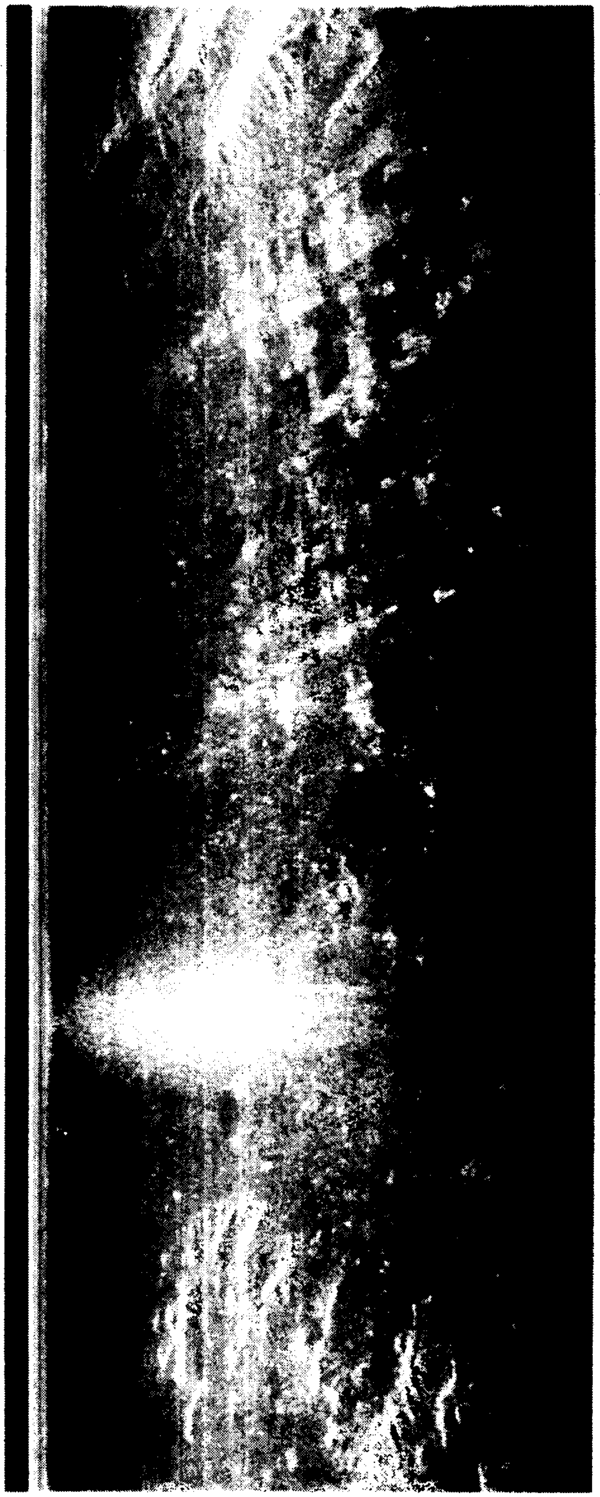

FIGURE 1.6.13 RADAR IMAGE OF PHOENIX GENERATED FROM DATA LINK/AMTE VIDEO

1.6.1.2 Imagery of Engineering Interest

Figures 1.6.14 through 1.6.20 have been selected to illustrate a number of system effects which are primarily of engineering interest, but which manifest themselves in radar imagery generated by a system of the 2355 design. Some of these effects can easily be reduced in magnitude through design changes which would probably be included in any future system design. Others are not so easily removed. The effects illustrated are the following:

- Effects on the imagery of prf changes, and both minor and major misalignments of the range gate with the returning video (Figures 1.6.14 and 1.6.15);
- Effects on the imagery of the response of the AGC feature to radical differences in the radar reflectivities of two or more extended terrain areas which are imaged by the radar (Figure 1.6.16);
- The comparative effects on the imagery of using either of two different receiver gain settings when the system is functioning in the fixed-gain mode (Figure 1.6.17);
- The effects of severe weather on the imagery (Figure 1.6.18);
- The appearance of azimuth and range ambiguities, and the relationships of their apparent locations to those of the reflecting physical objects which induce these ambiguities (Figures 1.6.19 and 1.6.20).

A brief discussion of each effect and its cause accompanies each imagery sample.

A. Effects of PRF Changes and Range Gate Alignment

On most passes, the prf at turn-on, which had been preselected on the basis of the best available tracking data, did not provide the optimum time-coincidence of the range gate with the returning signal; the alignment of the two was then improved by a human controller on the ground, who adjusted the prf on the basis of the appearance of the video being received over the Wide Band Data Link. One such adjustment was made at system time 24273.2 secs. ZT on Pass 8, from P/L step 14 to P/L step 13. The prf prior to the switch (i.e., on the right-hand half of Figure 1.6.14) was (8248 ± 1) pps, corresponding to an interpulse period of (121.24 ± 0.02) μsec; after the switch, the prf was (8281 ± 1) pps corresponding to an interpulse period of (120.76 ± 0.02) μsec. On the basis of the post-flight ephemeris and S-LOOK calculation of slant range it appears that the transmission of the n^{th} pulse preceded the recording of signal induced by reflection of the $(n - 17)^{th}$ pulse. Therefore, the effect of the change in prf on this occasion was to decrease by 7.5 μseconds the time interval between transmission of a particular pulse and the initiation of the sweep in which the reflected energy associated with that pulse was recorded. At the nominal incidence angle, this change implies a decrease of 1.1 n. mi. in the ground-range to the swath being imaged. The USGS map of Figure 1.6.14 shows this translation, as does the corresponding radar image; the apparent break in U.S. Highway 52 as imaged by the radar clearly illustrates this phenomenon. The translation as measured on the radar image is in agreement with the figure quoted above. Note that the illumination in the left half of the radar display is considerably more uniform that was that on the right; another subsequent one-step correction was necessary to achieve optimum coincidence of the range gate with the returning radar energy.

Another consequence of such a switch is a degradation (not apparent from the paper print) of azimuth resolution in the vicinity of the switch itself. Also, when data obtained via the Wide Band Data Link is used for image generation, an extensive loss of data sometimes occurs because of the properties of the time-averaging synchronizer used to provide sweep-synchronization for the ground-based recorder.

The situation depicted in Figure 1.6.14 is characteristic of the use of a nearly-correct prf. It is also of interest to observe the effect of a gross misalignment of the range gate with the returning video. Such a case is seen in Figure 1.6.15 generated from video collected

[redacted]

[redacted]

Figure 1.6.14 Single-Step PRF Change

in Pass 9 at system time 29561.6 secs. ZT. The system had been in P/L step 10 (prf = 8381 ± 1 pps, interpulse period = 119.32 ± 0.02 μsec) prior to this time (i.e., right portion of image), and was then commanded to P/L step 5 (prf = 8554 ± 1 pps, interpulse period = 116.90 ± 0.02 μsec). Prior to the switch, the transmission of the n^{th} pulse preceded reception and display of return attributable to the $(n - 17)^{th}$ pulse. A slight misalignment of range gate and video existed at this setting. At the new prf, the sweep was initiated far too early, while return due to the $(n - 16)^{th}$ pulse was in fact still arriving from the far range edge of the illuminated swath; the sweep then continued while the radar return strength decayed to a level dictated by the upper cutoff characteristic of the main elevation beam and then grew again as a result of energy from the $(n - 17)^{th}$ pulse, starting to appear at a level dictated by the lower cutoff characteristic of the main elevation beam. Finally, by the time energy due to the $(n - 17)^{th}$ pulse was returning from ranges within the main elevation lobe, the sweep was almost complete. The combination of a sufficiently narrow elevation beamwidth and lack of highly reflective targets near the beam edges caused the central part of the image to have negligible signal level.

The total effect is evident from an examination of the corresponding USGS map. The scene shown in the lower portion of the radar-generated print, to the left of the discontinuity, is a radar image of the terrain shown on the upper left hand portion of the USGS map, above the cross-hatched area. In each of these two segments, range decreases toward the top of the page. The scene shown in the upper portion of the radar-generated print, to the left of the discontinuity, is a radar image of the terrain shown on the lower left-hand portion of the USGS map, below the cross-hatched area. The upper edge of the radar print now corresponds to the lower boundary of the cross-hatch, and range increases toward the bottom of the page. Thus the upper and lower regions are reversed in sequence with respect to each other, but no other mirroring or inversion occurs. As was the case for the prf-switch illustrated in Figure 1.6.14, azimuth resolution is degraded in the immediate vicinity of the discontinuity.

The obvious effects of operating with an incorrect prf or of changing the prf are then the following:

1. Use of a prf which is incorrect by a relatively small amount (no more than 3 or 4 steps for the 2355 system) leads to a radar image of a strip which is displaced from that illuminated by the 3 db beamwidth, with the amount of translation determined by the magnitude of the prf error.

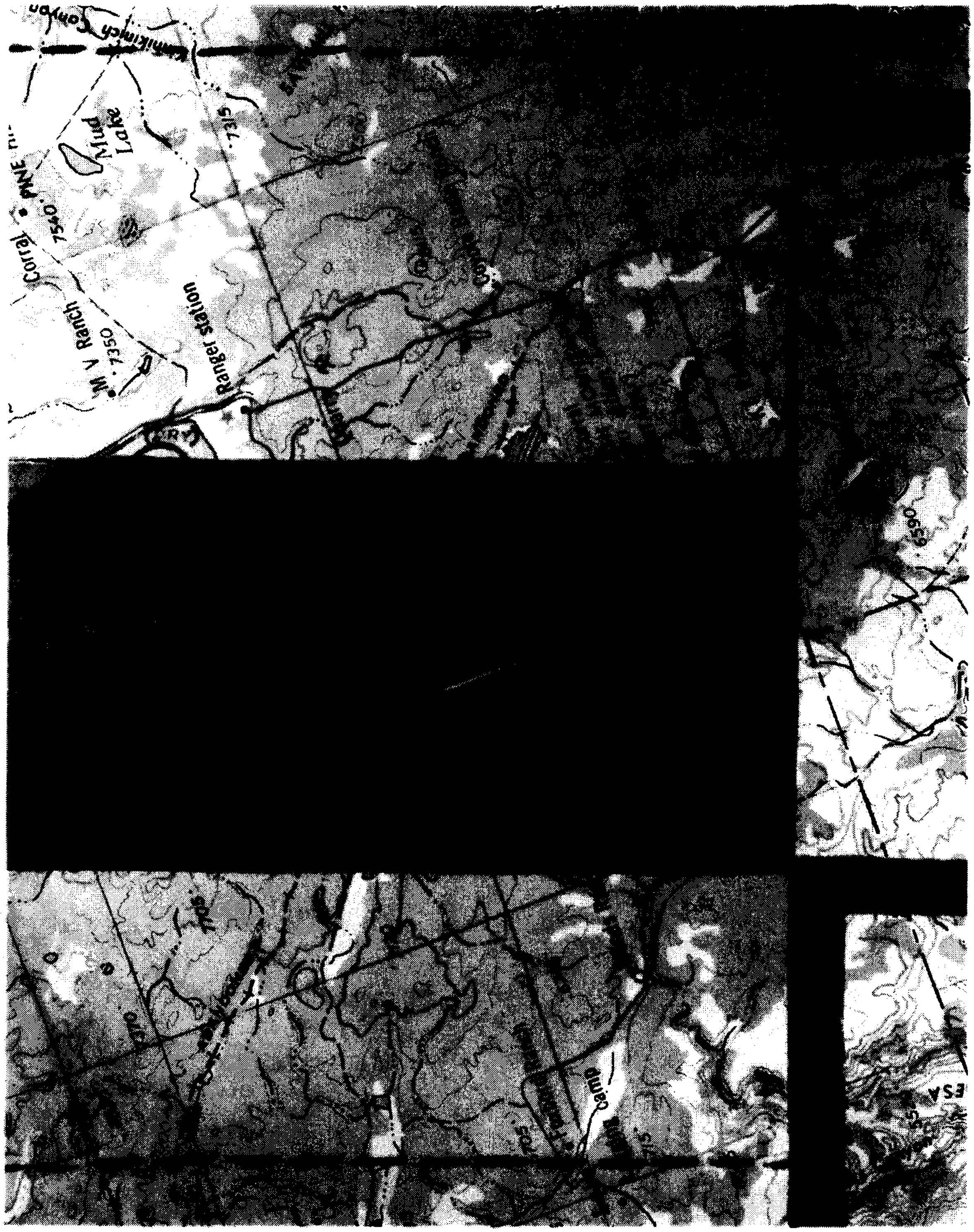

[redacted]

[redacted]

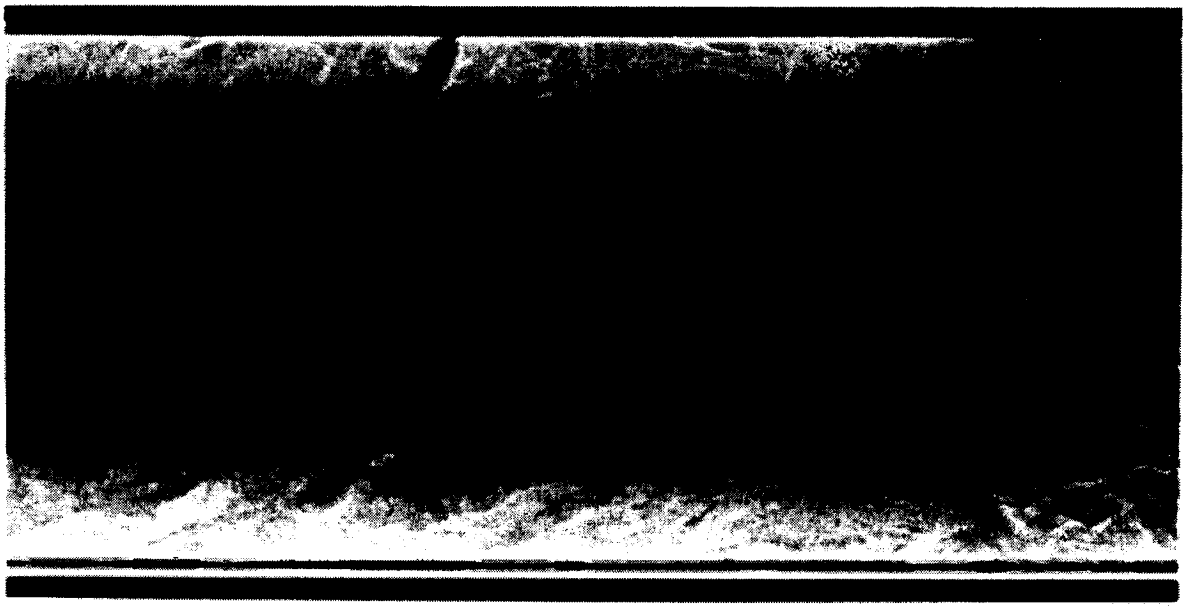

Figure 1.6.15 Five-Step PRF Change

The imagery has a signal-to-noise ratio which may vary drastically across the swath width, being higher on the side which corresponds to the intended coverage.

2. Use of a radically incorrect prf leads to imaging of the edges of the illuminated swath with moderate signal-to-noise ratio, and a total loss of imagery at the center of the illuminated swath.
3. Changing the prf translates the range of the swath being imaged.
4. Changing the prf causes a double-imaging of all targets which were being illuminated at the time of the switch, the intensity and resolution of each of the two images being dependent on precise target location but in any event being degraded as a result of the switch. (An example of the double-imaging has been found but is not presented in this report.)

The proper viewpoint toward the prf-selection problem is the following: in order to view a particular target area of interest, one must first guarantee that it is illuminated by the radar beam, and must then guarantee the energy reflected from that target area will be properly displayed and stored on the vehicle recorder. The first function required proper control of the attitude of the radiated beam; the second can then be achieved either through recording of all returning video, or through a proper prf selection. The latter feature relieves the storage requirements imposed on the system and also guarantees the transmitter will be inoperative while the returns of interest are arriving at the receiver.

B. Effects of Receiver Gain Changes

As was discussed under AGC effects above, the radar cross-sections of the various types of targets which one might wish to image range over several orders of magnitude. It is not practical to construct a receiver having a dynamic range adequate to permit imaging of such a collection of targets in a linear fashion. The elements which limit the system's dynamic range most severely (usually the recorder) are normally preceded by circuitry which attempts to control signal level in order to use the available dynamic range most effectively; an AGC is one such circuit, while a hard limiter is a second. The 2355 system incorporated an AGC which was in turn backed up by a number of fixed-attenuation steps; in the event of AGC malfunction, one of the fixed-gain steps could be chosen. The approximate effect of the AGC was to make the receiver gain vary inversely proportionally to the RF power received from a rectangular patch of terrain 10 n.mi. long in the range dimension and about 1 n.mi. in the azimuth direction, the range boundaries being coincident with those determined by the range gate. The AGC circuit responded with a time constant of about 30 milliseconds to changes in the level of this returning RF power. The rectangle reflecting the power was translated at the orbital rate of slightly under 4 n.mi/sec in the azimuth (along-track) direction.

A preliminary examination of the data indicates that isolated targets and target complexes contained within land masses did not induce severe responses in the AGC system; by and large, the extended terrain tended to dominate the average reflectivity and also accounted for some of its fluctuation. Strong AGC responses to land-water boundaries were noted, however. Figure 1.6.16 shows an excellent example of this behavior, which occurred during Pass 24. This image of the region around Wilderness State Park and the Straits of Mackinac, Michigan corresponds to system times 23936.9 through 23841.3 secs ZT on 23 December 1964. The prf selection was optimum at this time; as the satellite proceeded North along its trajectory, the radar beam was illuminating the eastern shoreline of Lake Michigan, and the AGC output was fluctuating in response to land masses and to ice on the Lake's surface. It is not possible to reconstruct a complete picture of the gain fluctuation from the TM data alone, since this was available only on the

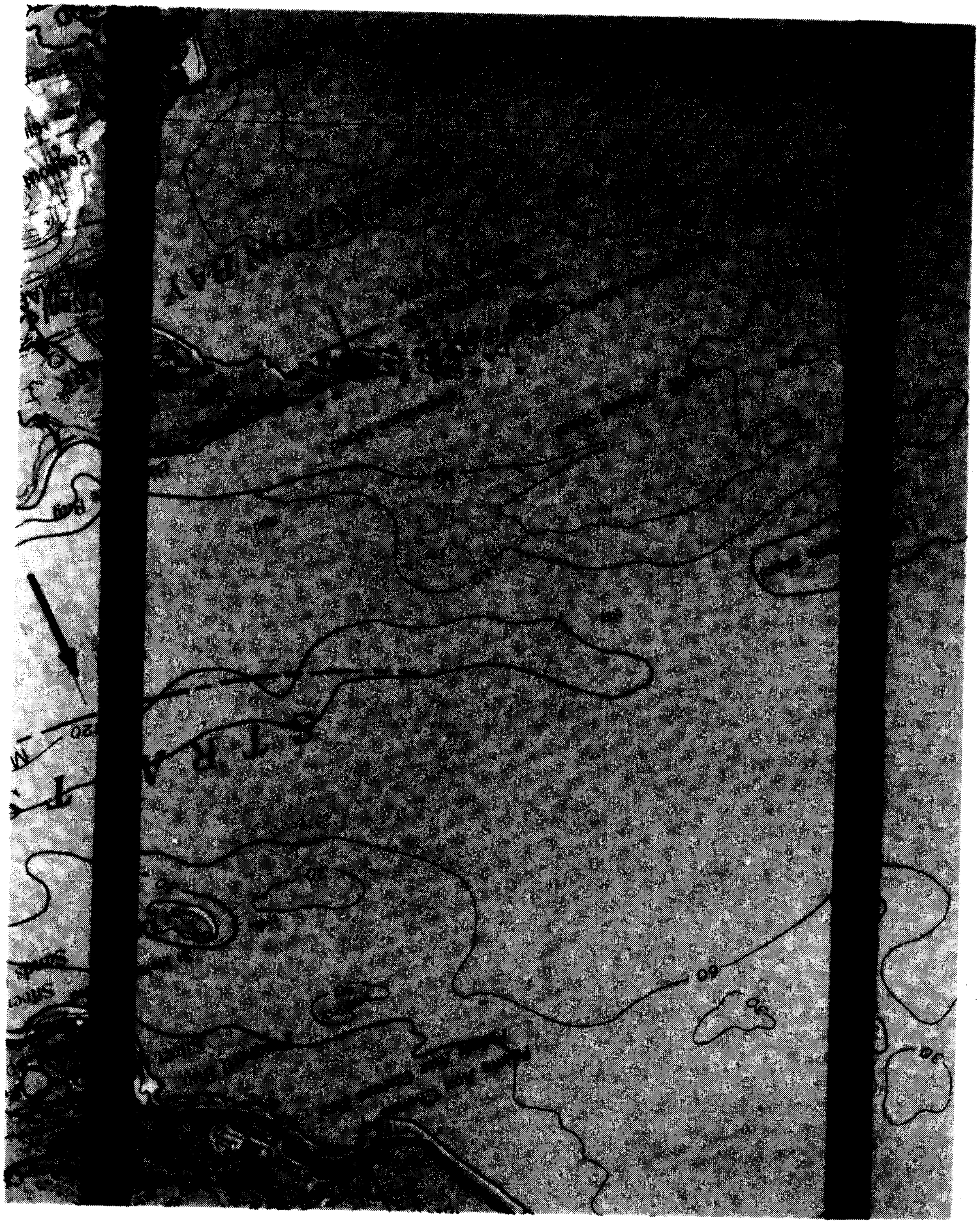

Figure 1.6.16 AGC Action

basis of one sample every 1.25 seconds. However, over the time interval of interest, the TM data shows a variation in return RF power from -90 dbm to -79 dbm, the latter value being reached on the first sample after passage into Michigan's Upper Peninsula and the offshore ice at the northern end of Lake Michigan (left-hand end of image). The variation in receiver gain during this time is estimated at 10 db, with maximum gain obviously corresponding to the "noisy" region midway between Wilderness State Park and the ice in the Straits and off Pointe Aux Chenes. A fixed-gain receiver properly adjusted to yield good ground-painting would have yielded an image of the water as devoid of return as are the water regions mapped concurrently with the land. Similarly, it might also have failed to show the wave structure seen in a previous image, Figure 1.6.10.

A comparison of the ground-painting achieved by the radar in two different fixed-gain settings is shown in Figures 1.6.17(a) and (b). This imagery was generated on Pass 41, and the gain change, from Position 4 to Position 3, occurred at system time 28735.9 secs. This change effected an increase of about 7 db in the gain of the receiver. The two prints are made from output transparencies which are processed to different exposure levels. Figure 1.6.17(a)

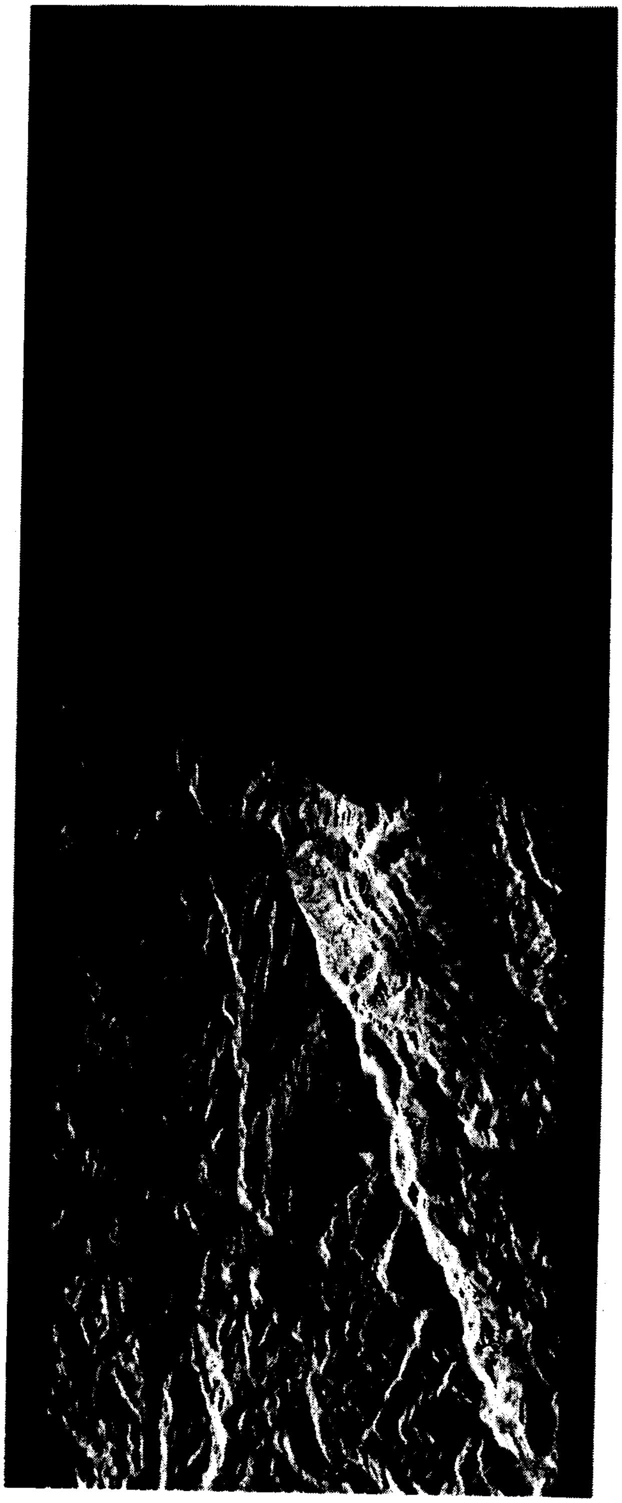

Figure 1.6.17(a) - Manual Gain Change - Processor Output Film - Exposure Fitted to Strongly Amplified Returns.

Figure 1.6.17(b) - Manual Gain Change - Processor Output Film - Exposure Fitted to Weakly Amplified Returns.

was processed to yield optimum ground painting on the left half of the scene (position 3), and the right half now appears underexposed.

Figure 1.6.17(b) was processed to yield optimum ground painting on the right half of the scene (position 4) and the left half appears quite heavily exposed. The left half of (a) can now be compared with the right half of (b) in order to permit a quality judgement to be made. A better judgement would be possible if both extended terrain and strong point targets were available on both sides of the switch; one would then look for the combination of good ground painting with minimum degradation or blooming of the point targets.

A radar image of similar terrain, viewed in the AGC mode, has been presented earlier in this report (Figure 1.6.7 of the section on Typical Imagery, above), and permits an interesting comparison. At the time of generation of Figure 1.6.7, the receiver gain, controlled by the AGC circuit, was equal to the gain of step 4 in the fixed-gain mode. Figure 1.6.17(b), left half therefore shows the image quality which would be obtainable in the AGC mode were the final video stages and the CRT recorder driven harder and allowed to limit more frequently than was the case. A more detailed examination of point-target returns obtained with the receiver in fixed high-gain modes will help to settle the question of degree of permissible limiting in future system.

Although the primary purpose of showing Figure 1.6.16 was to illustrate the AGC behavior, the image content is suffiently interesting to warrant some additional remarks.

Several forms of fresh-water lake ice are evident in this display of upper Lake Michigan, and the recent motion of one large area of floating ice can also be inferred. Grounded, shore-locked ice rather thoroughly masks the forms of the shorelines of Waugoshance Point and its island extensions. However, similar ice on the southern shore of Michigan's upper peninsula is more distinct from the land return in that area. Both land regions are wooded, but the AGC actions may have been different at these two times. The distinctly outlined dark area off Sturgeon Bay Point may represent new smooth ice; the strong-return area just north of it certainly gives an impression of crushed pieces, as does the brilliant return area located on the radar display where the word Straits appears on the map.

The breakage pattern of the large floe extending across the entire swath from St. Helena Island is extremely interesting, for it indicates the directions of the forces acting on the floe. The preliminary interpretation is that this 25-square mile sheet was formed in contact with the shore ice seen to its north, then broke off and moved away to the west or the south. Its eastern tip was caught by the island, causing the floe to break up under tension along its southern edge, but under compression along its northern edge. These stresses opened half-mile-wide leads into the one edge, while crushing and overlaying the broken pieces of the other. As must be the case for multiple tension fractures to occur, those farthest from the island "anchor" occurred first, as shown by their greater amounts of widening since fracture.

Other returns worth noting in this figure include navigational light structures at Vienna Shoal and off Waugoshance Island, plus a ship-like return about 2 n.mi. south of the latter.

C. Weather Effects

During Pass 16, the radar encountered the most severe weather experienced during the entire mission. Heavy rain was in progress along the California coast. There were scattered clouds at 700 to 1000 feet, and heavy overcast from 1400 to 2500 feet. The clouds were in layers extending to 35,000 feet. Winds were from the South, at somewhere between 10 and 30 knots when the image of Figure 1.6.18 was generated. The point of land is Pt. Reyes, California. Imaging of the water surface, wave structure, and breakers along the coastline is evident. The radar was in an incorrect prf step at this time, and the center of illuminated swath was totally offshore; the ground painting at the lower edge of the print is attributable to energy radiated from beyond the upper half-power point of the radar antenna. Intense reflection from active rain cells is to be seen along the shoreline.

The system time interval covered by this image is from 68705.0 to 68709.4 secs ZT. The RF power return falling within the range gate over this interval was of the order of -84 to -85 dbm, despite the misalignment of the range gate with the physical beam. The implied reflectivity of the sea surface is quite high compared with that observed on inland lakes, this being a consequence of the sea state due to the rainstorms and winds. It is worth noting, however, that wave structure is apparent even beneath the rain-cell images, and that the heavy cloud cover did not in any apparent way interfere with the imaging process. Some anomalous observations made elsewhere during this pass will be discussed further in [redacted] [redacted] evaluation report.

AC04306

6-200

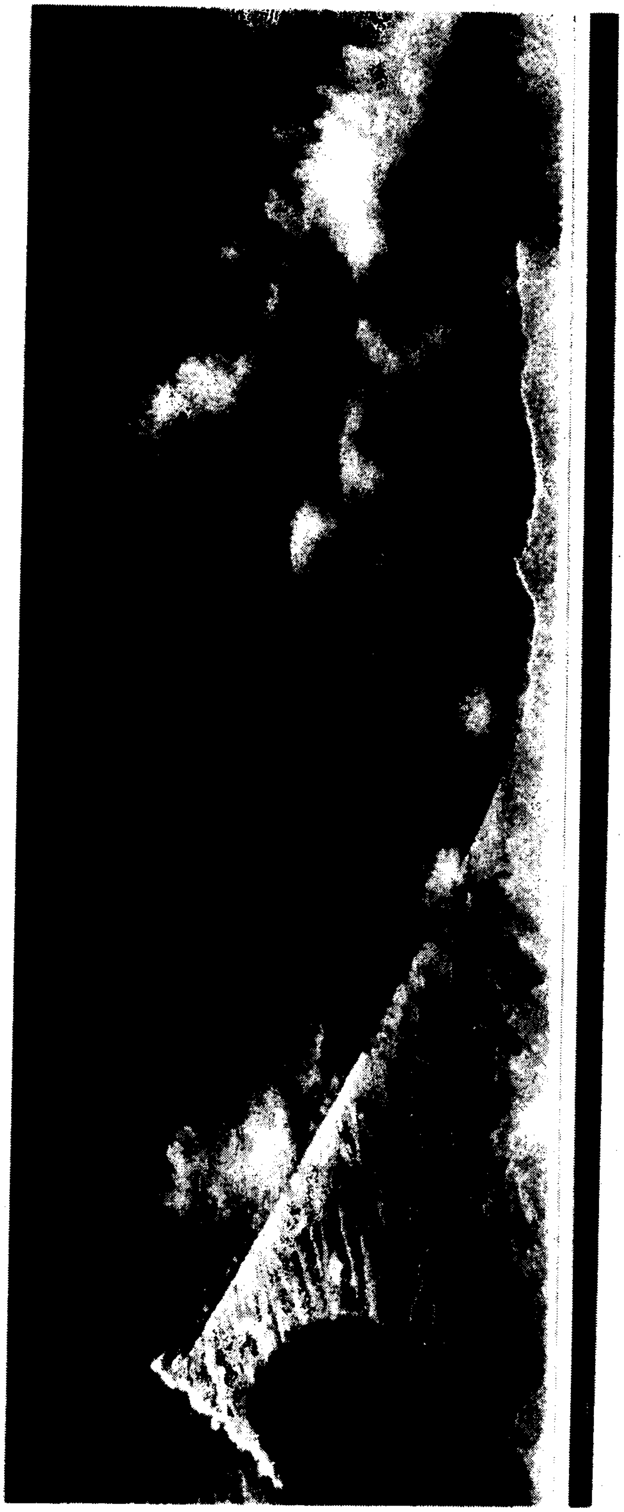

Figure 1.6.18 Rain Cells

D. Ambiguous Images

Under certain conditions, the radar imagery will contain target indications which are misplaced in azimuth or in range. The "ambiguous" target images are manifestations of the general "radar ambiguity problem" which will be covered in the [redacted] evaluation report, and which is a leading consideration in the design of satellite radar system. For the purposes of this report it is sufficient to say that strong reflectors will yield not only a target indication at the correct range and azimuth coordinates, but also at a number of other range and azimuth coordinate pairs. The energy associated with these ambiguous indications is always much smaller than the correct (non-ambiguous) indications due to these same targets, but is not necessarily smaller than the energy associated with the resolution cells upon which they are super-imposed. The only significant ambiguities for our purposes are the pair known as the "first focused azimuth ambiguities" and another pair known as the "first range ambiguities."

The first focused azimuth ambiguities corresponding to a point target at coordinates (X_1, R_1) will appear at locations

$$(X_1 + \Delta , R_1) \text{ and } (X_1 - \Delta , R_1)$$

as illustrated in Figure 1.6.19a. The energies associated with the three indications are denoted by σ_0 (the true response), σ_{-1} and σ_{+1}. The quantity Δ is given by

$$\Delta = \frac{\lambda R_1}{2v} f_p$$

where λ is the radar wavelength, v is the magnitude of the along-track component of the satellite velocity, and f_p is the prf in pulses/sec. If the receiver gain remains constant over a time interval long enough for the satellite to pass all three physical locations, then σ_{-1} and σ_{+1} are equal in magnitude; the parameters of the 2355 system were such that σ_{-1} and σ_{+1} should each have been about 40 db smaller than σ_0, provided the clutterlock was properly settled. No azimuth ambiguities have been found in regions where the gain remained unchanged over a sufficient time interval about the time of passage of a point target; such ambiguities would be difficult to detect.

An example of an azimuth ambiguity which was enhanced in level due to a sudden change in receiver gain is shown in Figure 1.6.19b; this image was generated on southbound Pass 30, as the southern shoreline of Lake Erie was being crossed at Cleveland. The system time interval corresponding to the image shown was 57470.4 to 57474.8 secs on 23 December 1964, the first shoreline encounter being at system time 57471.3. The gain of the receiver

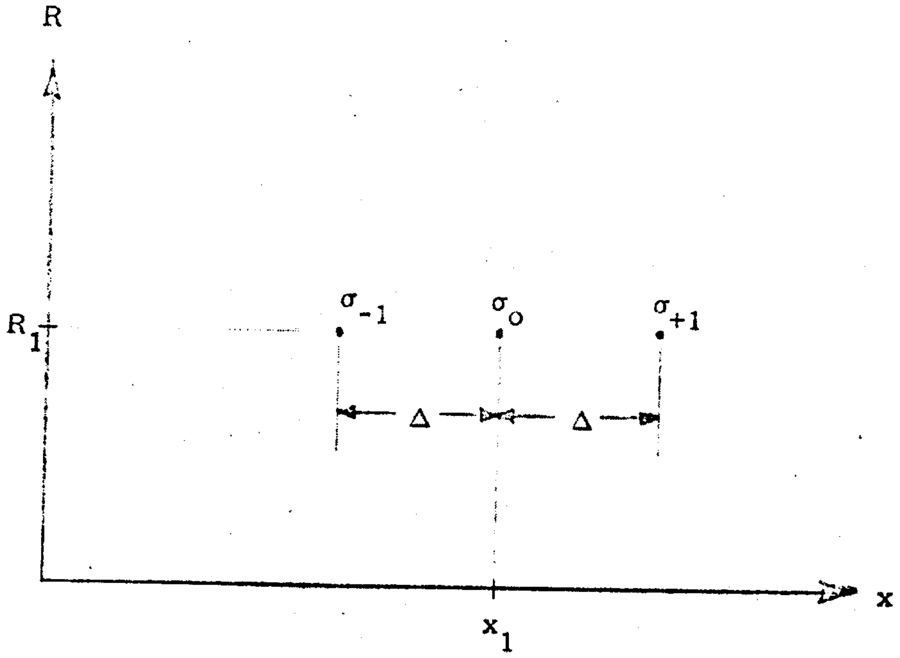

Figure 1.6.19a Azimuth Ambiguity Locations

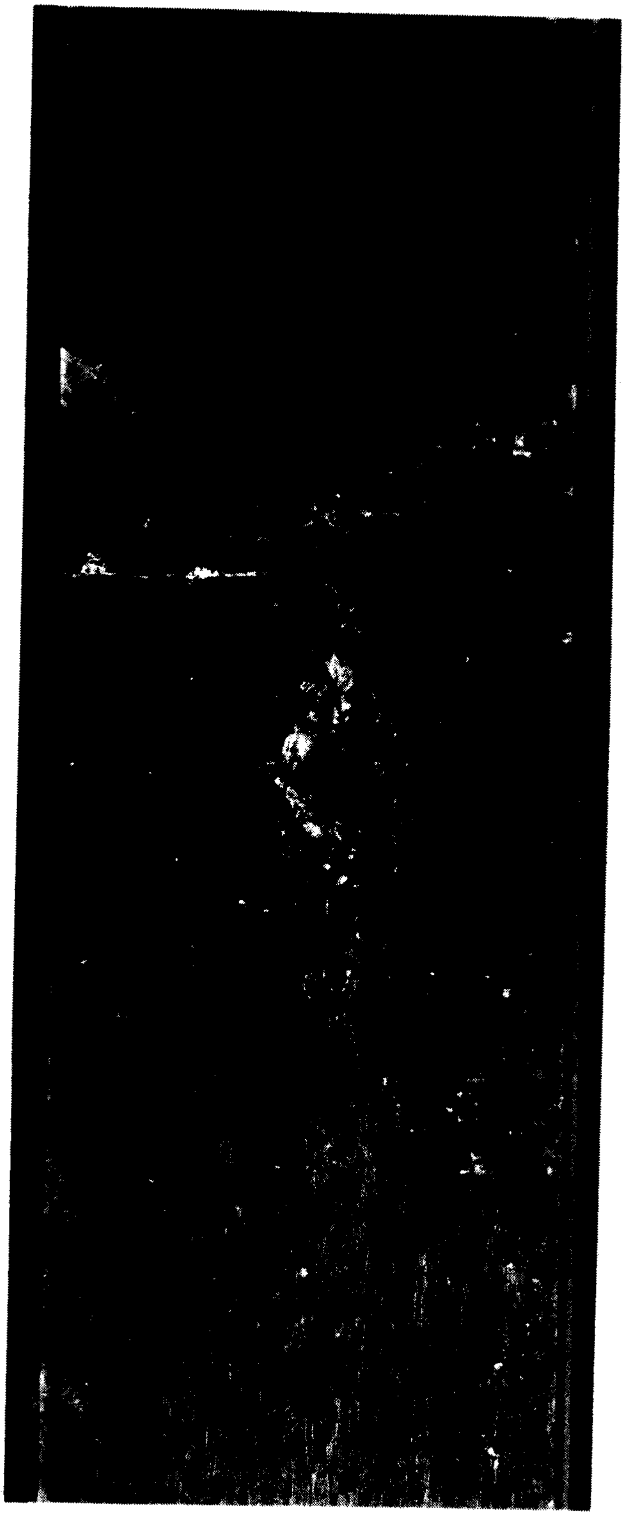

Figure 1.6.19b Azimuth Ambiguity

dropped sharply as the terrain being illuminated by the radar beam changed from the waters of Lake Erie to the city of Cleveland. The prf at this time was 8415 pps; at the center of the swath, the calculated value of Δ is 2.6 n.mi; Δ increases slightly, from the near-range edge of the swath to the far-range edge, by roughly 1 part in 25 for the parameters corresponding to this image. Figure 1.6.19b clearly shows, in Lake Erie, a set of point images which are a displaced and very slightly rotated replica of strong point targets on shore, The measured displacements agree with the calculation. The telemetered RF-power level over the lake was -89 dbm; over Cleveland, the arriving RF power increased to -74 dbm. Since this change would have led to a corresponding reduction in receiver gain of 15 db, the point-images on the lake were enhanced in energy by roughly this amount, hence to 25 db below the correctly positioned images. The clutterlock was behaving properly during this portion of Pass 30. Measurement of the relative energy levels of the true images and the ambiguous images has not been completed to date; however, it is unlikely that the 40 db ratio of true response to first focused ambibuity was actually achieved by the system. This latter speculation is based on visual examination of the true and ambiguous responses in output imagery.

Range-ambiguous returns may appear on the output imagery if strong targets at certain distances outside the desired swath are excessively illuminated. Ambiguous-range targets are imaged at their correct azimuth positions but at erroneous slant ranges, the slantrange error being

$$\epsilon_{R_s} = \frac{c}{2f_p}$$

where c is the velocity of propagation of the radar signal. In flat terrain, the ground-range error is related to the slant-range error by

$$\epsilon_{R_g} = \frac{1}{\cos\theta}\,\epsilon_{R_s}$$

where θ is the angle of incidence. Earth curvature introduces a slight error into this expression; terrain relief, especially in mountainous regions, introduces a much larger one.

Figure 1.6.20 shows an example of a radar image upon which ambiguous images of mountains were found superimposed. This image was generated on Pass 9, over the system time interval 29531.1 to 29535.3 secs ZT on 22 December 1964. The scale factors for this radar image are as follows:

Azimuth:	2.50 n.mi/inch
Ground Range:	4.27 n.mi/inch

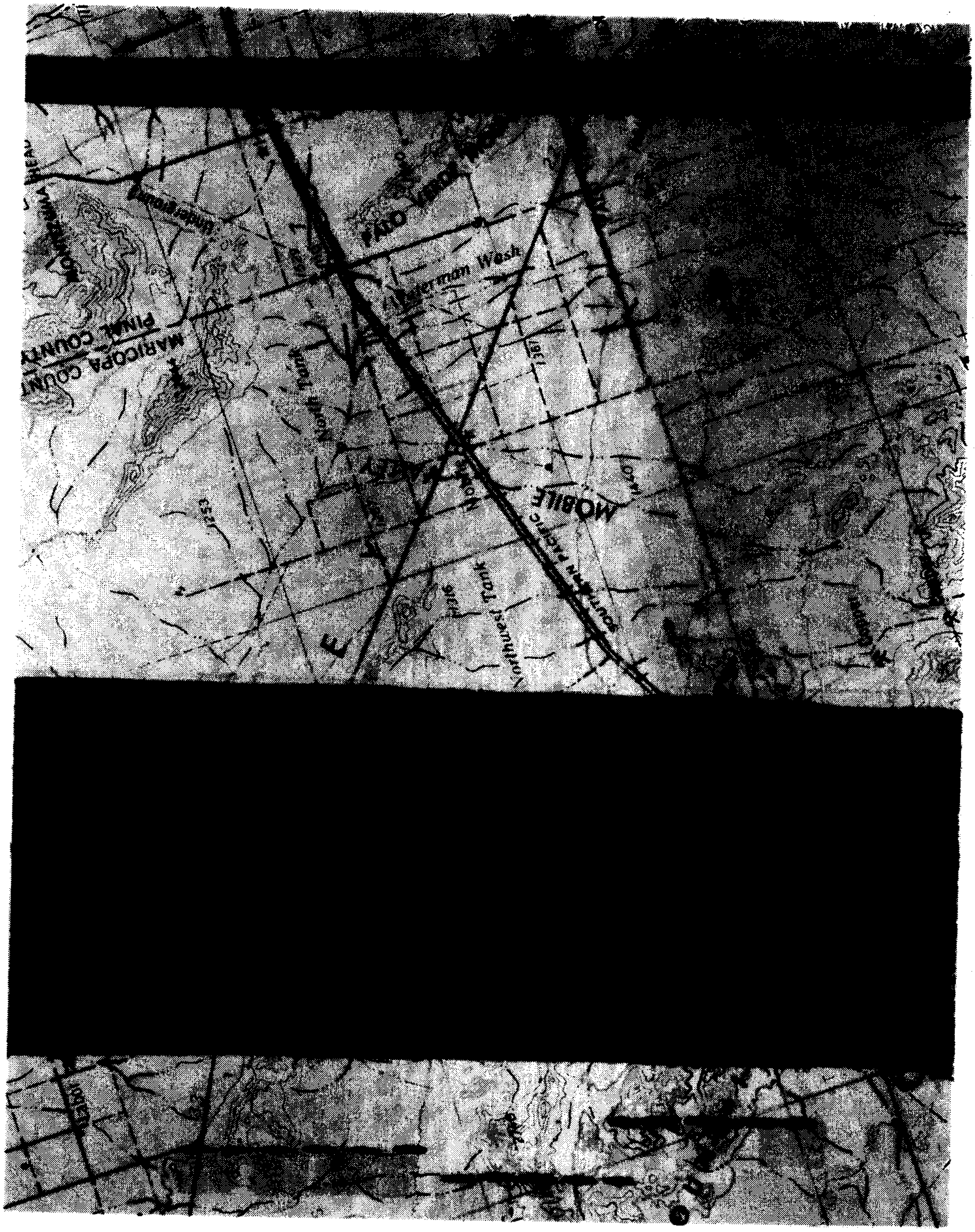

[redacted]

[redacted]

[redacted]

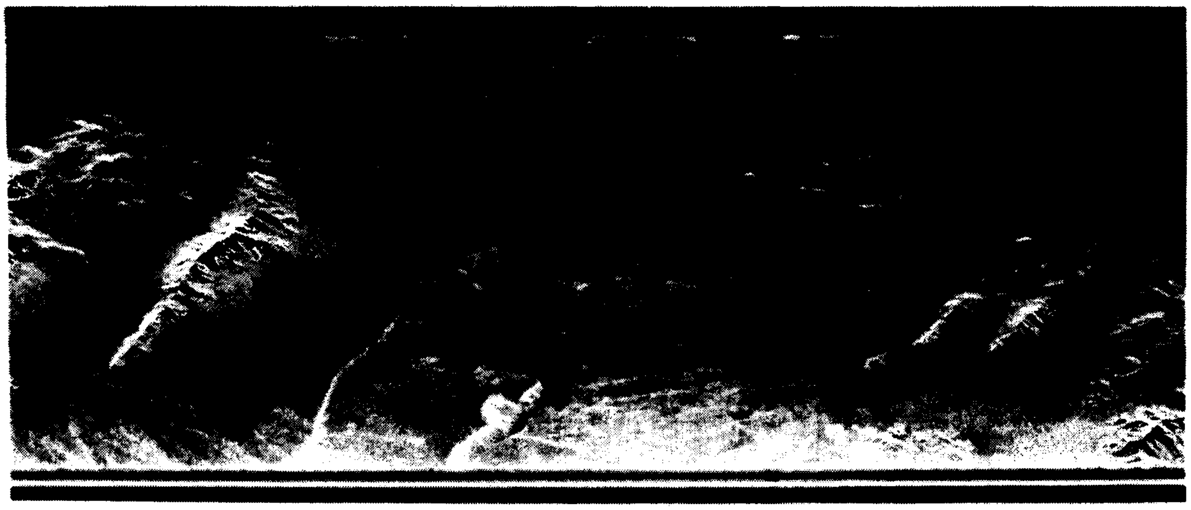

Figure 1.6.20 Range Ambiguity

The receiver's range gate was adjusted to record data from the strip above the cross-hatch, more or less centered on Mobile, Arizona. The range gate was somewhat misaligned with respect to the video; the peak of the elevation beam was probably centered on the upper edge of the cross-hatch, so that the mountains near the lower edge of the reproduced section of USGS map were reflecting excessive radar energy back to the receiver. The signal reflected from the mountain in response to the n^{th} pulse was reaching the receiver in time coincidence with energy reflected from the near-range (upper edge of swath) in response to the $(n + 1)^{st}$ pulse; both were, of course, accepted by the receiver, displayed, and recorded on the signal film. The resulting image shows the mountains displaced to the upper edge of the desired swath. The prf at this time was 8381 pps; neglecting relief, the displacement is calculated to be 16.5 n.mi. The height of the mountain and the change in incidence angle across this full width introduce an error of a few tenths of a mile into this estimate. The observed displacement is in reasonable agreement with the calculation. Careful comparison of the structure of the image versus the map contours also identifies these mountains as the source of these image elements which clearly are not derived from the flat terrain of the desired swath.

Figures 1.6.19b and 1.6.20 have illustrated the appearance of range and azimuth ambiguities. Such appearances were rare occurrences in the 2355 flight, and were only found where a radical receiver gain change or misalignment of range gate and video return enhanced their levels. However, the ambiguity problem places important constraints on radar parameters for satellite systems. Further consideration will be given to this problem in [redacted] [redacted] evaluation report. The illustrations are presented here primarily in the interest of completeness.

* [redacted] report which is referred to in several places above will be entitled [redacted]

1.6.1.3 The Resolution and Dynamic Range Test Array

Prior to the flight of 2355, a network of resolution test arrays was laid out in such a manner that, with high probability, one would be imaged during the first two days of operation. The test arrays consisted of radar corner reflectors of four different crossections which were geometrically deployed to permit estimates of azimuth resolution and ground-range resolution to be made over the dynamic range of the system. One such array was successfully imaged during Pass No. 8, at system time 24330.9 seconds on 22 December 1964. The test array was located on one edge of [redacted] The range/azimuth grid of the test array was slightly misaligned with respect to the range/azimuth grid generated as a result of the actual orbit. A sketch of the orientation with respect to the swath direction of the two larger sizes of corner reflectors is shown in Figure 1.6.21. The azimuth spacings are 7.5, 15, 30, 50 and 100 feet, whiel the ground-range spacings are 50, 85 and 200 feet. The resolution predicted on the basis of design parameters and pre-flight tests was 10 to 15 feet in azimuth and 70 to 80 feet in ground range. Figure 1.6.22 shows a pair of large-magnification prints of the reflector arrays as mapped by the radar system; Figure (a) is heavily exposed and shows both the 10,000 ft^2 and 3000 ft^2 reflectors, the larger ones being quite badly overexposed; while Figure (b), lightly exposed, shows only the returns from the 10,000 ft^2 ones. It is evident from the images that azimuth resolution was poorer than 7.5 feet but better than 15 feet, while ground-range resolution is estimated at 75 feet. The 100 ft^2 reflectors (and marginally, the 10 ft^2 reflectors) should have been above system threshold on a SNR basis; these are not detectable. The loss of the images of the 100 ft^2 reflectors may be attributable to the response of the AGC network to a strongly reflecting industrial complex (Dow Chemical Co.) which was mapped immediately prior to the reflector arrays. This point will be investigated further prior to publication of [redacted] flight evaluation report.

An independent estimate of resolution can be made through measurement of the two-dimensional response of the radar system to an isolated "point" target having a large radar crossection. Such targets were imaged in a number of instances. Careful measurement of the system response was made directly at the output of the optical processor; the half-power resolutions were found to be the following:

Azimuth:	10 feet between half-power points.
Ground Range:	72 feet between half-power points.

These results are in general agreement with those obtained via use of the resolution test array.

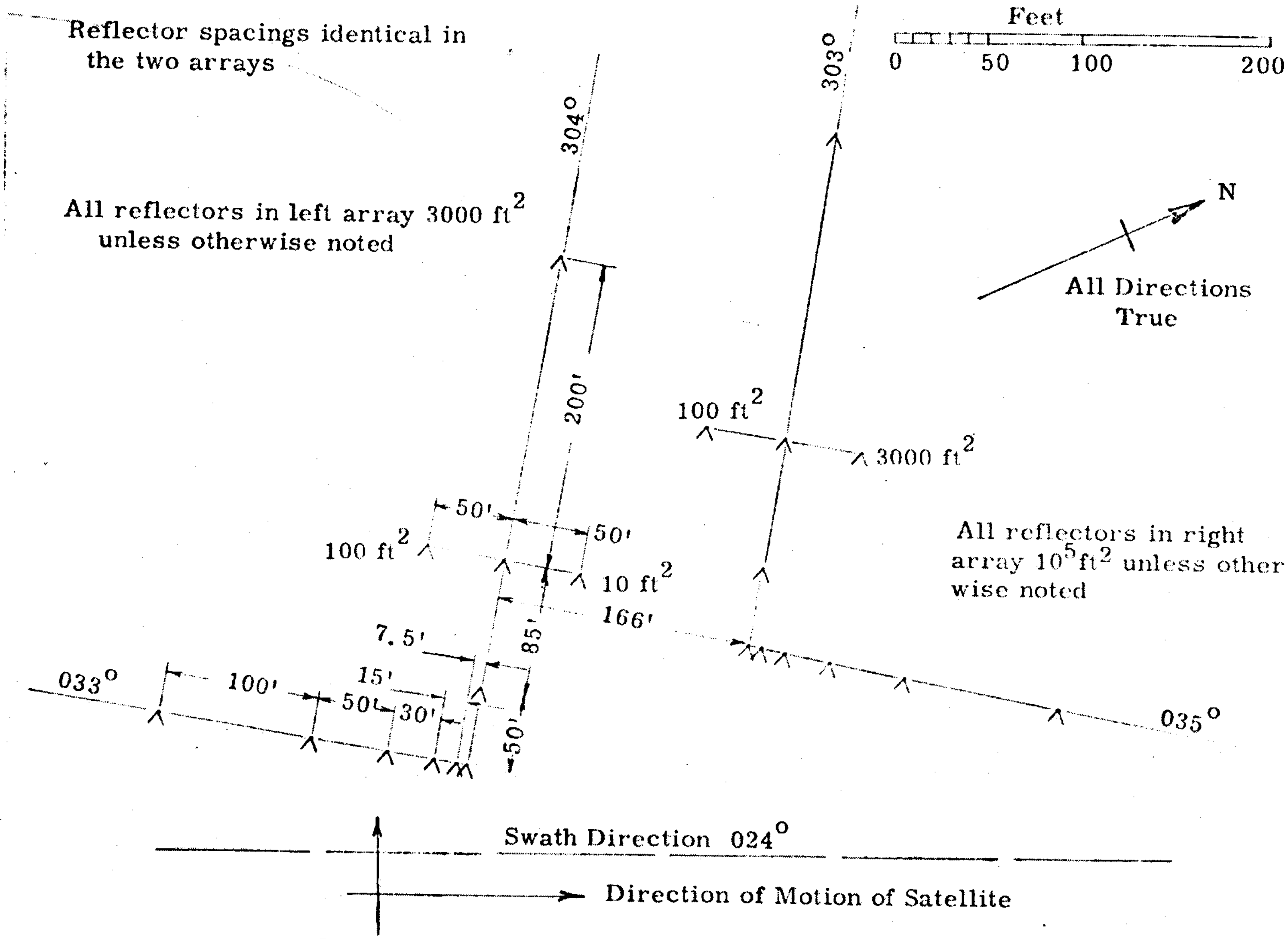
Reflector spacings identical in the two arrays

All reflectors in left array 3000 ft² unless otherwise noted

All reflectors in right array 10⁵ft² unless other wise noted

All Directions True

Figure 1.6.21 [redacted] **Test Array**

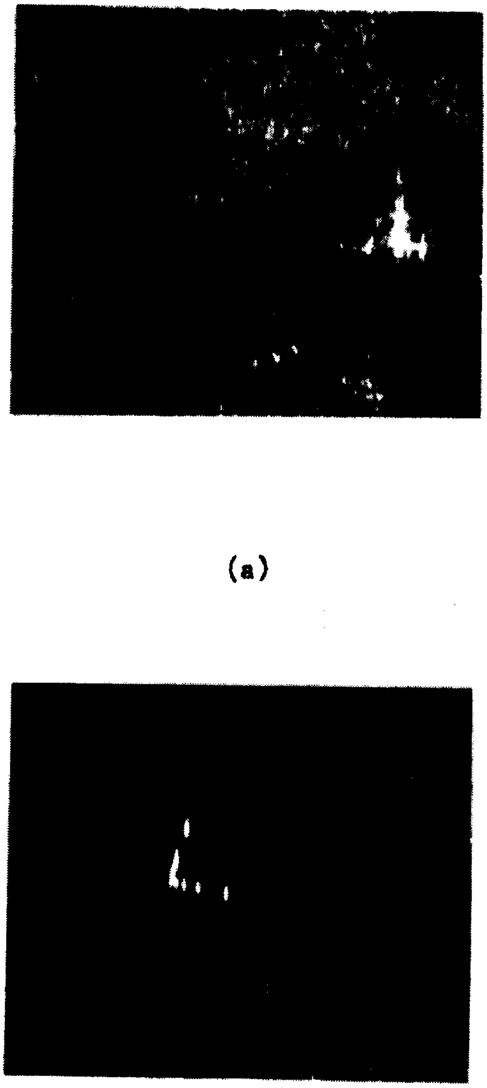

(a)

(b)

Figure 1.6.22 Output Images of Test Array

1.6.1.3 Image Quality Degradation

The image quality presented in Paragraphs 1.6.1.1 and 1.6.1.2 preceding, suffers degradation from that available at the processor output, as mentioned on Page 6-12.

To enable the reader to better evaluate a photographic enlargement of selected terrain, glossy prints of the following areas are included, with the reference pages listed for comparison with the smaller scale prints previously shown on semi-gloss paper:

Richmond, Virginia	Page 6-27
Wurtsmith AFB, Michigan	Page 6-35
Mothball Fleet, Wilmington, N.C.	Page 6-61
Pt. Reyes, California	Page 6-101

In addition, an enlargement of a section of the doppler history data film is provided, which supplements the smaller scale doppler print appearing in Volume II, Page 4-5.

1002306

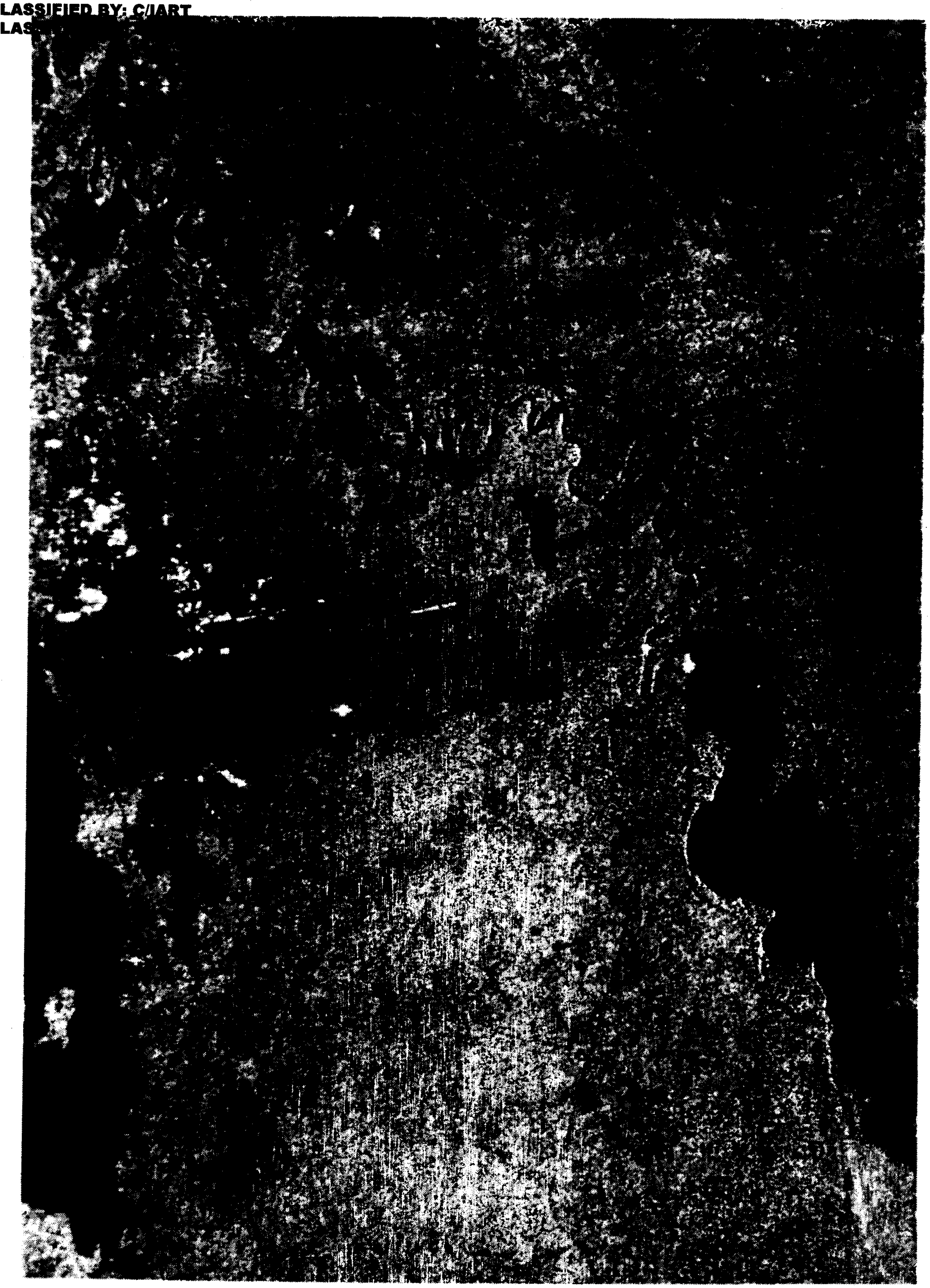

1.7 Conclusions and Recommendations

Conclusions The major conclusions that have been drawn from the flight of Vehicle 2355 are summarized as follows:

- The orbital flight satisfied the primary program objective by demonstrating that a satellite-borne synthetic-aperture radar system could generate a fine-resolution image of a portion of the earth's surface. All the program secondary objectives were also satisfied.

- The radar-image characteristics were very close to those predicted from the insertion of orbital-system parameter values into an analytic model whose validity had been confirmed previously with aircraft-borne systems.

- Because of the satellite's smooth trajectory, the imagery exhibited consistently fine azimuth resolution and uniform scale over image lengths of hundreds of miles. The achieved 10-foot azimuth resolution implies the realization of the large synthetic apertures required at the long ranges which are characteristic of orbital operation.

- The system proved its expected ability to produce radar imagery of a consistently high quality by day, by night, and through a variety of weather conditions; the conditions which prevailed in most of the swath areas would have prevented successful photographic or infrared imaging.

- The experiment did not produce any evidence of phenomena which would prevent future systems from realizing azimuth and ground-range resolutions on the order of 10 feet.
- The satellite-radar imagery contains many identifiable terrain and cultural features of likely value for strategic reconnaissance.
- The flight data strongly indicates that comparable radar images would be generated by aircraft-borne and satellite-borne radars which have similar resolutions and signal-to-noise ratios, and operate at similar depression angles. In particular, satellite borne systems are not subject to the resolution limitations normally imposed by platform instability in aircraft.
- Data recovered via a wide-band data link produced radar imagery which was only slightly degraded with respect to that produced from physically-recovered data.
- The criteria used in the design of the radar system provide a firm basis for the design of future satellite radar systems offering improved performance.
- The use of an electronic clutterlock for steering the synthetic beam was proven to be highly successful.

<u>Recommendations</u> It is recommended:

- That designs of future satellite-borne radar systems be based on the type of analytic model used successfully for this design, and upon the data obtained during this orbital flight.

- That future systems be designed to provide ground-range resolution more nearly equal to azimuth resolution, and to produce output images of higher signal-to-noise ratio.

- That the dynamic range requirements of elements of future systems be carefully reviewed on the basis of data collected during this experiment.

- That an evaluation be made of various means for post-launch adjustment of the radar beam's depression angle, in order to provide for viewing of pre-selected target areas.

- That future orbiting systems utilize improved techniques to assure time-alignment of the returning radar energy with the recorder range-gating.

- That an evaluation be made, with respect to their implications for orbiting systems, of various means for obtaining acceptable imagery over wider range intervals.

- That future experimental orbiting systems incorporate power sources which are adequate for extended-duration missions, as required for operational applications.

- That all future systems be provided with film time-coding to facilitate data evaluation.

- That the next flight of an orbiting system be instrumented to permit more frequent sampling of received signal levels and of clutterlock behavior, and more accurate monitoring of certain receiver and transmitter functions.
- That future systems incorporate available state-of-the-art improvements to provide an even more stable platform for radar imaging.

The reader is referred to the Goodyear Aerospace Corporation report recommendations for further specific comments pertaining to the radar payload.